Morphogenesis beyond in vivo

Authors: Yue Liu[1 *], Xufeng Xue[1], Shiyu Sun[1], Norio Kobayashi[1], Yung Su Kim[1], and Jianping Fu[1,2,3 *]

[1]Department of Mechanical Engineering, University of Michigan, Ann Arbor, MI, USA

[2]Department of Biomedical Engineering, University of Michigan, Ann Arbor, MI, USA

[3]Department of Cell & Developmental Biology, University of Michigan Medical School, Ann Arbor, MI, USA

*Email: umliu@umich.edu, jpfu@umich.edu

Abstract

Morphogenetic events during development shape the body plan and establish structural foundations for tissue forms and functions. Acquiring spatiotemporal information of development, especially for humans, is limited by technical and ethical constraints. Thus, both stem cell-based, in vitro development models and theoretical models have been constructed to recapitulate morphogenetic events during development. These in vitro experimental and theoretical models offer accessibility, efficiency and modulability. However, their physiological relevance often remains obscure, owing to their simplistic nature, which obstructs their applicability as faithful and predictive models of natural development. We examine existing in vitro experimental and theoretical models of various developmental events and compare them with the current knowledge of natural development, with particular considerations of biomechanical driving forces and stereotypic morphogenetic features. We highlight state-of-the-art methods used to construct these in vitro models and emphasize the biomechanical and biophysical principles these models have helped unveil. We also discuss challenges faced by the current in vitro experimental and theoretical models, and propose how theoretical modeling and in vitro experimental models should be combined with in vivo studies to advance fundamental understanding of development.

[H1] Introduction

During development, morphogenetic dynamics sculpts distinctive biological forms in animal bodies across species, length and time scales, and settings. Biological forms act together to support fundamental functions of life, such as breathing, moving and digesting. To decipher the mechanical forces that drive stereotypical morphogenetic events during development, substantial work has been conducted on animal models, revealing general mappings between molecular signaling and morphogenetic dynamics. Despite these successes, progress with animal studies remains constrained by the limited accessibility of spatiotemporal information in animal models, which obstructs detailed understanding of how biological signals are transduced into biophysical stimuli to shape tissue morphologies. From a pragmatic perspective, there are also uncertainties in applying animal-based knowledge for understanding human congenital disorders, owing to interspecies variations of morphogenetic dynamics. Furthermore, knowledge remains limited about how self-organization of morphogenetic cues and tissue forms can feedback to developmental signaling and cell–cell communication. Such signaling crosstalk is known to be important for controlling patterning networks to ensure the robustness and precision of development.

Beyond animal models, recent progress on development modeling based on in vitro-cultured stem cells, especially pluripotent stem cells (PSCs), provides an alternative tool to study development. These stem cell-based in vitro models generate multicellular entities that recapitulate cell lineage diversification, patterning and morphogenesis manifested in early embryonic development and organogenesis. Thus, stem cell-based models provide promising tools to study how endogenous and exogenous signals orchestrate tissue development[1-4]. In parallel, theoretical and in silico models have also been constructed to rationalize morphogenetic principles.

In this Review, by juxtaposing canonical development knowledge, stem cell-based models and theoretical analysis for some representative morphogenetic processes, we argue that a conjugation between high-fidelity in vitro models and theoretical study can advance understanding of morphogenesis with quantitative specificity, for both topological and conformational morphogenesis. In particular, stem cell-based models possess modulability, which can be further consolidated by a spectrum of bioengineering tools, and are thus ideal for interrogating how endogenous scales, exogenous stimuli and boundary conditions participate in morphogenesis. We further discuss some fundamental obstacles and challenges for in vitro development modeling, from both conceptual and technical perspectives. We envision that future studies of morphogenesis should go both in vivo and beyond.

[H1] Topological morphogenesis

The intricate topologies of an animal body constitute its structural basis for essential biochemical, biophysical and biomechanical processes and functionalities. For example, cavities enable substance exchange and transportation, and joints in the skeleton facilitate motion. Three representative morphogenetic events that alter embryo topology during early development are lumenogenesis, through which tissues generate internal boundaries, segmentation, through which tissues split apart, and folding, through which tissues deform and fuse boundaries (**Fig. 1**). These processes are driven by both bulk and interfacial behaviors at both tissue and cellular scales.

[H2] Lumenogenesis

Lumenogenesis is a fundamental, cavity-generating morphogenetic process that delaminates intercellular interfaces and generates a fluid-filled lumen **[G]**[5]. Lumenogenesis has been shown to be mediated by various mechanisms, such as hydraulic fracturing and coarsening during blastocoel **[G]** formation[6] and mesenchymal-to-epithelial transition **[G]** (MET) during secondary neurulation **[G]**[7]. In this Review we focus on lumenogenesis of peri-implantation epiblast **[G]**, leading to amniotic cavity formation (**Fig. 1A**). Mouse studies show that both apical constriction and integrin signaling from the basal membrane are required to drive epiblast cells to undergo polarization and reorganize into a rosette-like structure with a nascent central cavity[8-10]. As lumenogenesis progresses, E-cadherin is removed from apical surfaces of the epiblast through endocytosis and replaced by CD34 family antiadhesins; this process reduces intercellular adhesion and facilitates cell membrane separation. In addition, epiblast cell proliferation generates intermembranous pockets at the cleavage furrow **[G]**, which fuse with the central lumen, further increasing lumen volume and propelling its expansion.[9] Increasing embryo size has also been reported to induce apoptosis-associated formation of multi-layered and multi-lumen epiblast compartment, suggesting a size dependence in both morphology and mechanism of lumen regulation[11].

Epiblast lumenogenesis has been reconstituted through culturing mouse pluripotent stem cell (mPSC) aggregates in 3D Matrigel cultures (**Fig. 1A**)[8-11]. Lumenogenic mechanisms acting in vivo appear to operate in mPSC-based epiblast models[8-11]. In addition, an osmotic pressure gradient generated by ion pumps at the center of mPSC aggregates seems to drive lumen expansion[9]. Similar epiblast development models showing lumenogenic dynamics have also been generated using human pluripotent stem cells (hPSCs), with the lumenogenic dynamics promoted by actin polymerization but inhibited by actin contraction[12]. Formation and trafficking of a subcellular structure, termed apicosome, in hPSC-based epiblast models is proposed to promote cell polarization and central lumen formation[13,14]. Mechanical factors such as aggregate size[11,15] and matrix mechanics[16,17] also modulate

lumen structure and amniotic differentiation in hPSC-based epiblast development models. It remains to be explored how the location and number of lumen nucleation sites are determined within an originally amorphous epiblast or PSC cluster. This question can in principle be studied by modulating geometries of PSC-based epiblast models through bioengineering approaches.

As shown in both animal and in vitro models, epiblast lumenogenesis involves a range of cellular machineries. To regularize lumenogenic dynamics, a unified theory that integrates different mechanisms is necessary. Towards this goal, a minimalistic theory has been developed that considers both cross-membrane and paracellular transport of ions and water, highlighting the importance of pumping activities[18]. In another agent-based in silico model, reduced adhesion and apical repulsion at the center of epiblast compartment appear essential for lumenogenesis[19]. Because of the variety of mechanisms involved, an accurate account for all biophysical factors that nucleate nascent lumens and promote their expansions is non-trivial, and can benefit from quantitative characterizations on stem cell-based lumenogenesis models. Future theoretical efforts are needed to fully incorporate both subcellular mechanisms and cellular reorganization during lumenogenesis, a multiscale endeavor.

[H2] Segmentation

One of the most prominent topological features of the vertebrate musculoskeletal system is the segmentation of vertebrae by interfaces. Segmented topology of the vertebrae can be traced back to the process of somite **[G]** formation, known as somitogenesis, during embryonic development (**Fig. 1B**). Somites develop from a sequential and cyclic rostral **[G]** (R)-to-caudal **[G]** (C) segmentation process. During somitogenesis, somitic cells at the rostral presomitic mesoderm (PSM) reorganize into an epithelial rosette-like somite through MET, regulated by genetic factors, such as *TCF15*[20,21] and *PAX3*[22], and intracellular signaling molecules, such as small GTPases[23,24]. The forming somite contracts and delaminates from the rostral PSM through a ball-and-socket separation[25].

In a conceptual clock-and-wavefront model, the periodicity of somite formation is attributed to a molecular oscillator, termed segmentation clock, in PSM cells. Somite size is regulated by C-to-R gradients of morphogens such as FGF8[26,27]. The FGF8 gradient travels caudally during each segmentation clock period, and rostral PSM cells that experience FGF8 levels lower than a critical value (the 'wavefront' of the clock-and-wavefront model) initiate MET and form a rosette-like structure.[28] Animal models have provided finer molecular details of the clock-and-wavefront model. For example, in the zebrafish the segmentation clock periodically and locally inhibits Fgf/ppERK signaling and thereby dynamically modulates its relative slope to control the spatiotemporal segmentation process[29]. Apart from intracellular developmental signals, mechanical signals such as

external strain and surface tension also regulate boundary formation[30], length and left–right symmetry of somites[31].

Studying somitogenesis requires detailed spatiotemporal information of trunk development, which is challenging to obtain using mammalian animal models. To date, it remains elusive how upstream signaling dynamics is translated into MET-associated regulators and ultimately leads to new somite boundary formation. Other questions that remain incompletely understood include the origin of drastic interspecies differences in the number of somites and thus vertebrae, and the causes of somite segmentation anomaly that leads to congenital vertebral defects[32-34].

Stem cell-based in vitro models have been developed to recapitulate somitogenesis (**Fig. 1B**).[35-39] In these models, clusters of hPSCs embedded in 3D Matrigel undergo symmetry breaking and establish a R–C axis along which various somitogenesis-related dynamic events are recapitulated, including somite boundary formation, traveling waves of the oscillatory segmentation clock, spatially patterned lineage specification, and axial elongation[36-39]. Extracellular matrix and its concentration are shown to modulate the expression of genes associated with somite epithelialization[38] and structure[36]. Interaction between FGF activity and the segmentation clock is also observed in these models[39]. However, both segmented[37] and unsegmented[38] morphologies of somitic cells are reported in somitogenesis models from *HES7*-knockout hPSC lines (*HES7* is a segmentation clock gene). Furthermore, in vivo, the PSM tissue and forming somites experience mechanical confinement by neighboring tissues, a phenomenon which is absent in current in vitro models. Engineering mechanical boundaries in somitogenesis models might help reveal intrinsic biophysical determinants in somitogenesis.

Theoretical models have been established to describe the synchronization[40], mechanosensitivity[41] and clock-and-wavefront mechanism[42] of the segmentation clock. The periodic segmentation and lineage patterning dynamics are also recapitulated in silico, based on differential adhesion[43] and apical tension[44] mechanisms. In the differential adhesion model, a developing rosette-like structure forms from somitic cells due to mechanical repulsion between somitic cells and PSM cells, despite a lack of explicit modeling of epithelialization and reorganization of somitic cells in the forming somite[43]. In the apical tension model, apical constriction pulls epithelializing somitic cells away from the PSM and thus generates a new somite boundary.[44] In both models, mechanical interactions within the somite–PSM system drives new somite boundary formation and thus shares certain physical similarities with fracture in solids and the Plateau–Rayleigh instability of fluids.

Since there is limited knowledge about how intracellular signaling dynamics instructs somite boundary formation during somitogenesis, most theoretical models require empirical hypotheses and parameters to generate mechanical driving forces and induce somite boundary formation. These

limitations can now be addressed by leveraging the accessibility of stem cell-based somitogenesis models. For example, cell sorting observed in stem cell-based somitogenesis models[37] can be incorporated by theoretical models as a driving force for somite compartmentalization. Dynamic gene expression associated with the segmentation clock and formation of somite can also be quantified in stem cell-based somitogenesis models and compared with theoretical predictions.

[H2] Folding

During development, the embryo undergoes various folding dynamics by deforming and fusing boundaries to form cavities and thereby establish primordial organs such as the neural tube **[G]**. Neural tube is the embryonic precursor to the central nervous system. Following gastrulation **[G]**, the embryonic ectoderm undergoes neural induction, giving rise to the neural plate **[G]** at the dorsal **[G]** midline abutted by non-neuroectoderm tissues. Subsequently, the embryo initiates convergent extension, with the embryo body elongating along the R–C axis and shrinking along the medial **[G]**–lateral **[G]** axis, resulting in a reduction of the distance between the two lateral edges of the neural plate and thus facilitating its folding and closure process (**Fig. 1C**). Driven by cell shape change[45,46], cytoskeletal dynamics[47] and mechanical forces from adjacent non-neuroectoderm tissues, the neural plate starts bending, with its lateral edges elevating and creating neural folds. In mammals, bending of the neural plate occurs at specific locations in the neural plate, termed medial and dorsolateral hinge points. At these hinge points, the neural plate is anchored to adjacent tissues: the medial hinge point is anchored to the prechordal plate mesoderm and notochord, and dorsolateral hinge points are anchored to adjacent surface ectoderm of the neural folds. Thus, hinge points stabilize the neural plate during bending. As the opposing neural folds meet on the dorsal midline, they fuse progressively and form the neural tube. Defective folding of the neural tube leads to neural tube defects (NTD), one of the most common congenital anomalies[48]. To date, mechanical driving forces underlying the bending and closure of the neural plate — and the biological origin of these forces — remain debated, due to complexities in cellular mechanisms, boundary conditions and spatial heterogeneity.

Neural development models have been successfully developed based on 2D microprinted hPSC colonies, in which spatially organized neural induction and folding morphogenesis are induced. (**Fig. 1C**)[49,50]. Geometric confinement by non-neural epithelial tissues in these models induces folding dynamics of neuroectoderm tissues[49]. Greater neuroectoderm tissue size seems to hinder its folding and closure[49], supporting the importance of convergent extension of the embryo prior to neural plate folding in vivo. Defective neural plate folding occurs when either anencephaly **[G]** patient derived-PSCs[50] or NTD-related chemical drugs[49,50] are used in these models. How to establish in vivo-relevant

boundary conditions such as mechanical interactions with neighboring tissues remains an open challenge for modeling the folding and enclosure dynamics of the neural plate.

Theoretical and computational models have been developed to rationalize topology-defining dynamics of neural tube formation. Discretized models[51-53], including vertex models[53,54], which are usually 2D, simulate the neural plate as an assembly of cell-representing elements governed by specific rules that dictate their shape, motion and force generation. Such discretized models are thus compatible with multiscale modeling. In discretized models, cells in the neuroectoderm gradually adopt a wedged or trapezoidal shape due to apical constriction, leading to dorsal bending of the neuroectoderm. However, from these discretized setups, it remains challenging to study why and how bending deformation localizes and gives rise to hinge points. The large number of parameters of these models impose additional challenges in justifying necessary assumptions and extracting principal factors.

Continuum models of neural tube formation have also been developed[55-57] by abstracting cellular driving forces as intrinsic curvature, active tension and inelastic strain within the neuroectoderm. Tissue elasticity, conversely, resists folding of the neuroectoderm, owing to strain energy. Continuum models of tissue morphogenesis, in general, require inputs such as tissue stiffness, cell contractility and geometry, which can be obtained through either experimental characterization or coarse-graining of discretized models. In continuum models of neural tube formation, extrinsic forces from neighboring tissues are shown to mediate hinge point emergence and bending of the neural plate[55]. Disrupted cellular force generation and tissue geometry are also confirmed in continuum models to cause neural tube closure failure[58]. However, a notable difficulty in continuum models is the question of how to connect constitutive laws and parameters (especially those related to driving forces of folding) with experimentally identifiable cellular and subcellular machineries and regulatory pathways involved in tissue morphogenesis.

For both discretized and continuum modeling methods, future efforts are desired to directly connect modeling components and parameters with molecular and cellular machineries that can be perturbed either for prediction validations or identifications of potential therapeutic targets for medical intervention of NTD.

[H1] Conformational morphogenesis

During development, tissues and organs acquire their intricate conformational features, such as surface topography and aspect ratio, to define their apparent geometry and cell mass distribution. Development of such conformational features of tissues and organs often involves spatially heterogeneous and anisotropic

growth and remodeling, either at tissue surfaces or within their volumes. These conformational features are closely linked to organ functions, as exemplified by the crypt-villus morphology of the intestine, which is important for its absorptive function. A few typical conformational morphogenetic processes include wrinkling, in which tissue mass localizes quasi-periodically, branching, in which mass growth is restricted on selected sites, and axial elongation, in which mass accumulation concentrates unidirectionally within a single region. These processes all involve spatial patterns of both developmental signaling and mechanics and likely their interactions (**Fig. 2**).

[H2] Wrinkling

The intestine adopts a wrinkled crypt-villus morphology on its interior surface, with finger-like structures (villi) protruding into the intestinal lumen and flask-like structures (crypts) between the villi. This morphology effectively increases the intestine's surface area more than 10-fold[59] and serves as a mechanical basis of its absorptive function. Villus morphogenesis initiates during early intestinal development and arises from biomechanical and biochemical interactions between tissue layers lining the intestinal lumen. In chick embryos, the villus morphology is shaped by elastic mechanical instabilities during midgut development, which arise from differential growths between the epithelium–mesenchyme composite and its surrounding smooth muscle layer[60]. The villus morphology of the intestine further leads to local maxima of epithelial signals such as Shh at villus tips, which restrict intestinal stem cell distribution to the base of each villus[61].

However, in mouse embryos, neither the smooth muscle layer per se nor its confinement force is required for villus formation in the intestine[62]. Signaling molecules including Hedgehog (Hh)[63,64] and platelet derived growth factor (Pdgf)[65] secreted by pseudostratified intestinal epithelium, and bone morphogenetic protein (Bmp)[62] secreted by mesenchyme around the intestinal epithelium have been shown to drive mesenchymal cells to proliferate and form localized cell clusters, which might push overlying intestinal epithelium locally towards the lumen center and thus generate villi (**Fig. 2A**). However, it remains undetermined whether and how local clustering of mesenchymal cells leads to sufficient local mechanical forces for villus formation and whether a feedback loop exists between localized epithelial curvature and mesenchymal proliferation and aggregation. Given the notable interspecies differences in villus morphogenesis dynamics, it remains unclear whether similar phenomena occur during human intestine development[66,67].

After villus morphogenesis, crypts start to emerge between villi. Myosin II-dependent apical constriction leads to invagination of inter-villus epithelium, whereas subsequent basal constrictions on cells between villi and nascent crypts form hinges and thereby compartmentalize the crypts[68]. The

intricate coupling between biochemical signals and cell mechanics that coordinates crypt-villus patterning and morphogenesis remains to be fully elucidated.

hPSC-based in vitro models have been successfully developed to recapitulate lineage specification and morphology of early-stage intestine developent[69-71]. Embedded in 3D cultures, hPSC-derived small intestine organoids show a pseudostratified epithelium surrounded by mesenchyme, which later acquires villus-like involutions that protrude into organoid lumens[69]. Mesenchyme-free intestinal organoids could also be developed from hPSCs, but without obvious villus morphology[70]. Mouse intestinal stem cells have also been used for organoid development with crypt formation (**Fig. 2A**)[72-75]. In mouse intestinal organoids, as in mice, myosin II-induced apical constriction, leading to local wedge-like cell shape, promotes crypt invagination[72-74]. Crypt invagination in mouse intestinal organoids occurs simultaneously with local cell fate specification events[73]. Additionally, lumen volume reduction driven by osmotic gradient and transcellular water transport appears to promote crypt morphogenesis in mouse intestinal organoids[72]. Cell migration from crypts to villus regions, which contributes to gut epithelial renewal[76], seems to be controlled by a tension gradient around crypt boundary. However, mouse intestinal organoids could develop crypt-villus structures without a mesenchymal niche[77], despite theoretical models based on in vivo studies that ascribe villus morphogenesis to the formation of mesenchyme clusters. It will be important for future hPSC-based intestinal organoids to control and manipulate epithelium–mesenchyme interactions and examine whether morphogenetic mechanisms known to function in animal intestine development would still operate in the context of human development.

Villus morphogenesis in chick embryos has been theoretically formulated as a minimization of elastic strain energy for gut tissues under differential growth. In this theoretical model the differential growth initiates wrinkling instabilities and successfully produces lumen surface topographies at different chick embryo development stages[60,78-81]. In contrast, murine villus morphogenesis is postulated as a Turing system in which Bmp ligands and their inhibitors develop spatial patterns via a Turing mechanism, and the Bmp pattern further drives chemotaxis and thus clustering of mesenchyme cells[62].

Crypt morphogenesis has also been computationally modeled with both continuum[79,81] and cell-based[82-84] methods. It has been shown that cell proliferation, contraction and shape change could lead to local invagination and produce a crypt-like structure by deforming the epithelium[79,81,83]. In continuum models, mechanical instability is treated as the major contributor for crypt morphology, whereas cell-based models include additional considerations of cell fate patterning, which generates localized deformation through lineage-dependent cell shape and behavior changes. Nevertheless, more biological specificity is required before juxtaposing such computational results with

experimental observations[85]. Cell lineage specification and distribution have also been mathematically modeled[82], and stem cell division in crypts is shown to minimize the time for crypt development[84].

Together, the coupling between mechanical morphogenesis, biochemical signaling and lineage patterning is still a major challenge in theoretical and computational modeling of crypt-villus morphogenesis. Signaling activity can spatially mediate cell behaviors such as contraction, proliferation and shape variation, and thus drive mechanical deformation. Reciprocally, tissue morphology and mechanics can in turn affect distributions and patterns of signaling activities. Therefore, it is necessary to simultaneously account for the biophysical and biochemical interactions between neighboring cells and tissues and explicitly address interspecies differences, in order to fully elucidate morphogenetic forces that shape the crypt-villus morphology in the intestine.

[H2] Branching

Branching morphogenesis is a ubiquitous process shared across plant and animal species. For example, it shapes the lung by establishing a fractal tree-like airway network to enable efficient air transport and exchange. Following the first branching bifurcation of the respiratory diverticulum **[G]**, which gives rise to two primary lung buds, airway branching morphogenesis continues until well into childhood and generates 300–400 million alveoli **[G]** in each mature lung[86].

At its early stage, the mammalian lung consists of an epithelium and an encasing pulmonary mesenchyme into which the epithelium branches. Patterns of branching in vivo have been classified either as domain branching, in which daughter branches develop in rows along the length of a parent branch, or bifurcations, in which daughter branches form on the tip of a parent branch[87]. Signaling molecules and regulatory networks involved in lung branching have been studied extensively[88-91], and morphogens such as Fgf10, which drives lung bud growth, and Shh, a regulator of Fgf10, have been identified.

However, physical regulation of branching morphogenesis is less understood[92]. It has been shown in ex vivo models that a stereotypical pattern of airway smooth muscle derived from the mesenchyme at budding sites is necessary for shaping both domain branching and bifurcation, by driving the epithelium to grow only in branching directions (**Fig. 2B**)[93,94]. Branching has also been observed for mesenchyme-free lung epithelium treated with Fgf10[95], suggesting an innate self-organizing property in lung epithelium for branching dynamics. Localized Fgf10 expression, however, has been shown dispensable for lung branching morphogenesis[96]. Together, given these seemingly contradictory observations, it remains unclear how the biophysical and biochemical signals from the lung epithelium and mesenchyme and their interactions control the location and pattern of

branching sites and the number of daughter branches, and mediate their orientations after their budding.

Lung bud organoids have been derived from hPSCs to mimic early lung development with branching morphogenesis (**Fig. 2B**)[97-100]. Embedded in 3D cultures and supplemented with signaling molecules including FGFs, endodermal cells derived from hPSC clusters rapidly expand and form branching tree architectures with a minimal presence of mesenchymal cells[97], consistent with an innate branching potential in early lung epithelium. Lung bud organoids have been used for modeling diseases[97,99] such as Hermansky–Pudlak syndrome. Although lung bud organoids do not mature in vitro, they still represent useful experimental tools to investigate early-stage airway branching development. However, efforts are needed to improve the fidelity of in vitro models, as some lung bud organoids do not produce branching morphology at all[101-103].

Various theoretical formulations have been proposed to account for branching morphogenesis. Based on the premise that branch growth pattern can be instructed by localized biochemical signaling, Turing models, in which interactions between diffusible Fgf / Shh molecules lead to patterned Fgf10 activities, have been employed to compute spatial patterns of signaling activities on the surface of a lung bud and thereby predict branch outgrowth sites[104,105]. Nevertheless, no bi-directional coupling between signaling activities and mechanical growth has been established. It is thus unclear whether a feedback loop exists between signaling localization and growth-induced curvature.

Mechanical interpretations of branching morphogenesis have also been proposed by drawing analogies between airway branching and mechanical instabilities such as buckling[106], which attributes branching morphology to mechanical instability generated by the growth of lung epithelium and the confining microenvironment, and provides a viable explanation for mesenchyme-free branching. Stochastic modeling has also been adopted to analyze spatial branching morphologies, revealing that neighboring duct density might promote branching termination by inhibiting tip growth and suggesting the existence of competing interactions between neighboring branches[107]. To date, most theoretical modeling efforts attempt to rationalize branching morphogenesis through a single source of physical driving force, yet the complex and seemingly contradictory experimental observations suggest the existence of a multilayered regulatory network — potentially with redundant or interacting components — contributing to branching patterns.

[H2] Axial elongation

Early vertebrate development entails an axial elongation along the R–C axis, involving coordination of different developmental events, such as maintenance of a progenitor domain, cell proliferation, and

cell motility. After primary neurulation, a major contributor to caudal axial elongation of the embryo body comes from a pool of proliferative neuromesodermal progenitor **[G]** (NMP) cells, the maintenance of which requires both WNT and FGF signaling[108-114]. NMP cells are bipotent and can both contribute to caudal spinal cord development and thereby drive its elongation, as well as give rise to highly motile caudal PSM cells. Motility of each PSM cell appears unoriented but shows a C-to-R (high-to-low) gradient, which is thought to cause unidirectional tissue growth, in analogy to particle diffusion under a temperature gradient (**Fig. 2C**)[115]. Interestingly, a gradient in mechanical property, from the fluid-like caudal PSM to solid-like rostral PSM, is also reported.[116] Moreover, mechanical interactions, including compression between axial tissues and PSM, and pushing force exerted by axial tissues on caudal NMP progenitor domain, are shown to coordinate the elongation of axial tissues and PSM (**Fig. 2C**)[117]. Nonetheless, specific factors that control the rate and duration of axial elongation and therefore the body length of embryo are still unclear. How the progenies of NMP cells contribute to the development of caudal spinal cord and PSM cells in the context of human development also remains an open question. Addressing these questions requires quantitative information about the biophysical environment of NMP cells and their activities at the cellular level, which in turn requires lineage tracing and biomechanical characterization of in vivo tissues.

Axial elongation has been shown in many PSC-based embryoids, including gastruloids[118-120], trunk-like structures[121], somite models[36-39,122] and neural tube organoids (**Fig. 2C**)[123]. These embryoid systems predominantly adopt gel embedding and WNT activation in their protocols, with a NMP progenitor domain localized at the elongating end, confirming its pivotal role in axial elongation. As axial elongation proceeds, the R–C axes of the embryoids are established with patterned HOX gene expression. Genetic perturbation of *TBXT*, a marker of mesodermal lineage, disrupts unidirectional elongation and caudal fate specification in neural tube organoids[123], consistent with mouse mutants in which *TBXT*-knockout leads to defective trunk morphogenesis[124,125]. Given the compatibility of embryoids with live imaging, they can be used for quantitative tracking of cell proliferation, motion and organization during axial elongation. Embryoids with both neural tube-like and somite-like structures are also valuable for investigating lineage bifurcation of NMP cells. The amenability of embryoids for mechanical characterizations further facilitates extraction of mechanical parameters and studies of mechanical interactions between different elongating tissues and migrating cells.

Theoretical and computational models have been constructed to understand axial elongation of vertebrate embryos. By modeling PSM cells as Brownian particles with random motility, it is suggested that geometric confinement together with PSM cell addition from the NMP compartment can physically promote axial elongation[126]. To investigate the mechanical implications of caudal Wnt signaling, tailbud cells are also modeled as self-propelled particles. It is suggested that a reduction in

cell flow coherence caused by disrupted Wnt activity could lead to cell jamming in the tailbud and thus defective elongation[127]. Nevertheless, more theoretical modeling efforts are required to understand axial elongation. For example, the synergistic elongation of different caudal tissues such as spinal cord and PSM is orchestrated by cell activities and tissue–tissue interactions at the extending front. Understanding these requires considering the caudal architecture of the elongating embryo. Furthermore, coordination between local biochemical signaling and cellular behaviors also needs to be established to quantitatively recapitulate their dynamic coupling.

[H1] Deconstructing morphogenesis

Morphogenesis of a developing embryo is a highly self-regulated process in which each step is meticulously and stereotypically controlled, suggesting the existence of well-curated governing principles in each tissue to ensure their correct morphologies. In examination of morphogenesis within an individual tissue, herein we deconstruct the principles into three principal aspects, namely endogenous scales embedded in a morphing system, exogenous stimuli superimposed over tissue body, and boundary conditions enforced by the extracellular environment or neighboring tissues (**Fig. 3**). If tissue morphogenesis can be rationalized as a mathematical system $\mathcal{D}[u] = f$, in which u denotes the state of a morphing tissue, the endogenous scales effectively characterize the operator $\mathcal{D}$ that describes interactions within the tissue. Exogenous stimuli instantiate f which depicts the background signals distributing inside the tissue domain, in analogy to the body force in a mechanical system or the distributive source or sink in a diffusion system. Together with boundary conditions acting on tissue peripheries, these factors form a closed system through which tissue morphogenetic dynamics can be quantitatively studied. Note that initial conditions are excluded from discussions in this section because they arise from either preceding developmental processes or artificial system setups and thus do not pertain to morphogenesis-governing cellular or tissue mechanisms.

[H2] Endogenous scales

Arising from interactions among resident cells within each tissue, endogenous scales depict the most fundamental driving force for their self-organization. As a regulatory mechanism for morphogenesis, upstream biological activities such as gene expression first lead to spatial patterns of intercellular activities, which are further translated into local mechanical activities of cells such as proliferation, contractility and changes in cell shape or mechanical properties. Mechanical activities of cells then provide physical driving forces to deform tissues and thereby shape their morphology. Through this process, two sets of endogenous scales would emerge, one associated with signaling activities and the

other associated with mechanics, which are interconnected through mechano-transduction[128]. Endogenous scales include intrinsic length and time scales and show correlations with cell or tissue characteristics such as physical properties, geometries, and dimensions, usually through certain scaling laws. The relevance and significance of these spatiotemporal scales can also depend on the system hierarchy of interest.

Spatial and temporal scales induced by biological signaling, driven by interaction and transport of soluble factors, depend not only on tissue geometry and physical properties such as transport rates, but also on interactions between cells and signaling molecules and the structure of signaling regulatory network (**Fig. 3A**). If the signaling mechanism involves two species of counter-interacting molecules, namely an activator with low transport rate and an inhibitor with high transport rate, the activator tends to accumulate locally and thus generates a heterogeneous pattern called a Turing pattern, which has been theoretically studied and reviewed extensively[129-131]. As a reaction–diffusion model, the Turing mechanism introduces intrinsic length scales such as the ratio between diffusivity and reactivity. Such intrinsic length in zebrafish germ layers is reported to be scalable with tissue dimension, rather than a constant, to ensure a proportional embryo pattern and normal development[132]. Therefore, extended Turing and reaction–diffusion models have been developed to investigate the emergence of robust size-insensitive patterning[132-134]. Turing patterns are associated with a variety of pattern formation in biological structures such as seashells[135], fish skin[136], and fingerprints[137], and is conceived as a governing mechanism of many spatially repetitive morphogenetic events such as villification[62] and branching[138]. Differential signaling behaviors between cells on tissue boundaries and those in bulk also introduce a length scale. For example, BMP signaling is restricted to border cells in mouse epiblast development due to BMP receptor localization on their basolateral surfaces[139], which leads to an edge-sensing length scale. Signaling activities can also result in time scales. For example, the rates of molecular regulation at the cellular level may provide a temporal pace for cellular activity, whereas the rates of long-range signaling interaction, such as molecular transport and degradation, could introduce characteristic time scales at the tissue level. The leading difficulties in justifying signaling-induced scales, however, include identifying associated signaling molecules and their interactions, quantifying their biophysical and biochemical parameters such as intercellular transport rates and intracellular regulation, and elucidating emerging crosstalk between signaling activities from different sources across different scales, which require experimental models accessible for both genetic manipulation and high-resolution live imaging.

Mechanical scaling, which describes the transition from mechanical driving forces to tissue shape, is sensitive to tissue mechanical properties and geometries (**Fig. 3A**). Within a mechanically stimulated biological body, mechanical energy is generated both on the surface, characterized by

properties such as surface energy, and in the bulk, characterized by properties such as modulus or viscosity. The ratios between surface and bulk quantities naturally define some length or time scales related to processes involved in topological boundary formation such as segmentation[31] or fracture in biological structures[140]. When polarized cells adopt a wedge-like shape, as in neural plate folding[45,46] and intestinal crypt invagination[68], an intrinsic curvature and therefore a length scale are activated. If elastic instabilities are triggered, tissue mechanical properties together with tissue dimensions would introduce a characteristic wavelength into the system. A common scenario where this length scale dominates is differential or inhomogeneous tissue growth, exemplified by villus formation in chick intestine[60] and looping of chick gut tube[141]. Together these length scales describe how cells are spatiotemporally displaced and sculpt tissue structures. The major difficulty in examining these underlying scales is in identifying the corresponding driving forces, which requires visualization of dynamic cellular behaviors at the single-cell resolution and biomechanical perturbations and characterizations in situ. Implementing these experimental methodologies on mammalian embryos in vivo remains a significant challenge.

Compared to their in vivo counterparts, embryoids and organoids usually provide superior manipulability and therefore stand out as promising systems to probe endogenous scales (**Fig. 3A**). With tissue dimension being an easily controllable parameter, size effects have been demonstrated on lineage development trajectory[142] and morphogenesis in embryoids and organoids (such as epiblast lumenogenesis, neural tube closure and intestinal crypt formation)[11,49,72]. With regard to signaling-driven scales, a BMP-stimulated spatial pattern of hPSC differentiation, as a 2D model of human gastrulation, has been demonstrated to occur through a reaction-diffusion mechanism[143]. Furthermore, using the same system, the edge-sensing length scale of BMP signaling can be mathematically modeled with a diffusion theory[139,144]. Similarly, cell mechanics has been shown to induce an edge-sensing length scale in a hPSC-derived neuroectoderm patterning model[145]. As another example of mechanics-induced scaling, biomechanical characterizations and theoretical analyses of mouse intestinal organoids reveal basic mechanical scaling laws between crypt morphology and geometric parameters of intestinal lumen such as spontaneous curvature, lumen volume and tissue thickness[72]. In terms of time scale, dynamics of the segmentation clock has been recapitulated and quantified across different species using species-specific PSCs[146-150]. Interspecies difference in segmentation clock period appears to correlate with biochemical reaction rates[148] and thus metabolic rates[146] and ultimately the embryogenesis timespan[147], which may provide hints about the fundamental timescale governing embryo development. However, the physiological relevance of endogenous scales embedded in in vitro models, which can be sensitive to the model architecture, is yet to be determined. It will be of interest for future work to elucidate the conditions for each scale to be

dominant through theoretical modeling, targeted modulations of in vitro models, quantitative comparisons between in vitro and in vivo phenotypes, and as such demonstrate the applicability of endogenous scales derived in vitro.

[H2] Exogenous stimuli

Exogenous stimuli such as extrinsic morphogens or mechanical cues can also instruct morphogenesis (**Fig. 3B**). In developing embryos, morphogens are synthesized by specialized cells or tissues within specific regions, generating spatial morphogen gradients in their environments through transport[151,152]. Morphogen gradients essentially provide a coordinate system with length scales to instruct spatially informed cell lineage development and morphogenetic movements through its slope and local intensity, which is also referred to as positional information[153]. For example, WNT and FGF signals generated at the embryo caudal tail bud result in C-to-R gradients of these potent developmental signals[108,154]. In parallel, somites in the trunk synthesize retinoic acid, the concentration of which is thus highest in the trunk and become lower towards the rostral and caudal ends of the embryo[155,156]. These morphogen gradients instruct lineage patterning along the R–C axis and are involved in regulations of morphogenetic dynamics such as embryo elongation and somitogenesis by inducing spatially graded cell activities such as motility, polarization and proliferation[108,115]. Similarly, positional information shapes the development of a limb along its proximal–distal axis, imposed by FGF signaling, and along its R–C axis, imposed by retinoic acid and SHH signaling[157,158]. Extrinsic mechanical stimuli such as tissue stiffening[159] and stiffness gradients[160] have also been reported and correlated to morphogenetic cell migration[159,161]. Nonetheless, given the technical difficulty in modulating their heterogeneity in in vivo models, it remains challenging to quantitatively characterize exogenous stimuli and establish spatial mapping between stimulus patterns and local morphogenetic events.

In vitro models have been successful in directly recapitulating heterogeneous exogenous stimuli (**Fig. 3B**). When lumenal hPSC cysts on coverslips are exposed to exogeneous uniform BMP4 stimulation, the lateral cyst wall obstructs permeation of BMP signals, leading to a medial–lateral (low–high) BMP activity gradient on its bottom surface. This graded BMP activity results in patterning of the non-neural epithelium on the periphery and neuroectoderm at the center of the cyst bottom, where neural folding dynamics is further induced[49]. Exogenous morphogen gradients have also been generated by microfluidics for modeling amnion–epiblast symmetry breaking[162], germ layer patterning[163] and neural plate patterning[164]. Thus, in vitro models with controlled exogenous stimuli can be useful for inferring dynamic formation of embryo body axes[151]. Exogenous mechanical stimuli with predefined spatial patterns have also been superimposed on 2D embryoids. For example, cell

fate can be spatially regulated in 2D gastruloids[165] and patterned neuroectoderm tissues[145] through local stretching and mechanotransduction. In these systems, patterns of exogenous stimuli are directly controllable, thereby enabling quantitative mapping between local mechanical stimuli and cellular behaviors, a significant technical advantage compared with in vivo models.

[H2] Boundary conditions

Molecular and mechanical interactions often take place at tissue boundaries, which define another component regulating morphogenetic dynamics within a tissue (**Fig. 3C**). Biochemically, a tissue boundary can provide a local source or sink for signaling molecules. Mechanically, tissue boundaries can define a spatial domain within which tissue morphogenetic activities proceed[128]. For example, physical confinements from the neural tube, epidermis, intermediate mesoderm and endoderm underpin the unidirectionality in PSM elongation[126]. Active force signals can also develop on tissue boundaries, such as the tensile margin between embryonic and extraembryonic tissues which drives gastrulation in avian embryos.[166]

In in vitro tissue cultures, boundary conditions are highly modulable, which facilitates investigations of their roles in tissue morphogenesis. The most prevalent boundary conditions implemented for in vitro models hitherto can be roughly categorized into three types (**Fig. 3C**). First, under a free boundary condition, both tissue growth and morphogen diffusion are unconstrained, as seen in free-floating tissue cultures. This boundary condition is probably most relevant to pre-implantation embryo development[167-169]. Second, under a tractile boundary condition, tissues experience mechanical interactions at tissue boundaries while chemical signals can still diffuse freely, as in 3D tissue cultures using natural or synthetic ECM. Such 3D tissue cultures provide an anchoring environment required for cellular activities such as migration, contraction and mechanotransduction without prohibiting exogenous chemical signal modulation. Third, under a solid boundary condition, neither tissues nor morphogens can pass through the boundary, as exemplified by tissues cultured on a solid surface. Such solid boundaries enforce spatial confinement and/or guidance for tissue development. Combinations of different boundary conditions have also been implemented[15,162,170]. Based on their modulability, different boundary conditions can be tested on the same tissue to uncover how they mediate tissue development and morphogenesis. Notably, none of the three boundary conditions, either individually or combined, fully recapitulates the biomechanical and biochemical complexity at tissue–tissue interfaces in vivo. To address this limitation, tissue–tissue co-culture models and multi-tissue embryoid systems have been developed[121,171]. It remains to be determined what the functional roles are of tissue–tissue interfaces in mediating tissue morphogenetic dynamics and how they can be effectively recapitulated in vitro.

[H1] Engineering morphogenesis

There are many bioengineering tools available for adoption in in vitro models for high-precision modulation, opening new possibilities for probing morphogenetic mechanisms[2]. Unlike conventional cultures in which cell colonies or 3D tissues are surrounded by uniform biochemical and biomechanical cues, it has now become possible to apply bioengineering tools to engineer tissue geometry, exogenous stimuli and extracellular environment, with designed spatiotemporal specificities down to the scale where morphogenesis is relevant. Doing so not only enables multiscale mechanistic investigations but also effectively improves experimental throughput and reduces variability between assays (**Fig. 4**).

[H2] Engineering geometry

One of the most effective and straightforward approaches to probe endogenous spatial scales is to modulate tissue geometry. Controlling tissue geometry can define the dimension and shape of cell colonies and thereby provide an initial and/or boundary condition for progressive morphogenetic dynamics. Based on soft lithography[172,173], the most common bioengineering methods to regulate tissue geometry include surface pre-patterning and micro-well confinement. In surface pre-patterning, adhesive islands with pre-designed patterns are generated on 2D surfaces onto which cells can adhere and thereby form colonies with desired geometries[49,165,174,175]. An example of surface pre-patterning is micro-contact printing (μCP), which facilitates customization of adhesive island patterns on a variety of cell culture surfaces such as glass coverslips, polystyrene dishes and polydimethylsiloxane (PDMS) (**Fig. 4A**)[172,176,177]. To develop stamps required by μCP, prepolymer of elastomer such as PDMS is poured and cured over a master with relief surface features fabricated by microlithography. Next, the stamps are coated with adhesive molecules and pressed against an activated surface to enable transfer of adhesive molecules from the stamps to cell culture surfaces to produce adhesive patterns.

To regulate tissue geometry in 3D, microwells in which cells can form 3D aggregates with target size and shape are widely used (**Fig. 4A**)[178-183]. Apart from commercial sources, microwells can be produced with elastomers via techniques like those used for μCP stamps. Microwells can also be fabricated with biological gels through micro-molding, in which elastomeric stamps with desired tissue architecture in bas-relief are used to mold gels[179,183,184]. Such geometrical regulation can be extended to develop 3D scaffolds with complex interior structures (**Fig. 4A**)[185,186]. Furthermore, bioprinting offers a powerful approach to generate initial tissue geometry with arbitrary conformation and topology (**Fig. 4A**)[186].

Geometric regulation on in vitro models allows efficient probing of endogenous scales encoded in morphing tissues. In 2D hPSC cultures, modulating colony geometry helps identify the

tension-mediated gastrulation-like phenotype[165]. By embedding mammary epithelial cells in 3D trenches of various shapes inside collagen gels, it has been shown that tissue geometry could instruct distribution of autocrine inhibitory morphogen signals and as such determine locations of and spacing between branching sites[179]. With similar geometric regulation methods, local geometry of mouse intestine tissues is found to induce a gradient in cell spreading and associated YAP activity, leading to crypt-villus lineage patterning and morphogenesis[183]. Via direct control of tissue size and shape, it is now possible to expose morphogenetic mechanisms that respond to or originate from tissue geometry and scale.

[H2] Engineering stimuli

The impact of exogeneous stimuli can be simulated and investigated through various engineering approaches. Signaling stimuli can instruct local cellular activities and convey inter-tissue communications during morphogenesis. To recapitulate spatiotemporal patterns of biochemical and biomechanical signals, a variety of bioengineering tools have been employed in organoid and embryoid cultures (**Fig. 4B**). To introduce localized sources of morphogens, morphogen-loaded microbeads have been incorporated into embryoid bodies to drive heterogeneous differentiation of PSCs[187,188]. Microfluidic technologies have also been used to generate defined morphogen gradients within cell cultures by engineering molecular diffusion patterns[163,164,189-191]. In these microfluidic platforms, cells are usually cultured in a confined space while different molecules are supplemented from different boundaries of the culturing space, forming a stable morphogen gradient pattern in the cell culture via passive diffusion. For example, when hPSCs are cultured in a micro-chamber with its two opposing sides adjacent to two channels, one supplemented with BMP4 and the other with SHH agonist, dorsal–ventral **[G]** (D–V) patterning is imposed on neuronal cells differentiated from hPSCs, mimicking neural patterning along the D–V axis[190]. Another microfluidic device for generating a linear morphogen gradient uses a serpentine channel gradient generator to create a quasi-linear WNT activator gradient over hPSC-derived neural tissues for their R–C regionalization[164]. To create a more drastic morphogen gradient, hPSC clusters can be anchored on the interface of two micro-channels supplemented with different morphogens. With BMP4 supplemented in one of the channels and no morphogen in the other, a spontaneous amniogenesis-like symmetry breaking in the hPSC cluster is induced[162]. However, confined space within microfluidics can lead to undesired mechanical interactions between developing tissues and device boundaries, a non-trivial limitation that precludes the use of microfluidics for long-term tissue cultures. More recently, optogenetic tools have also been used to locally control morphogenetic processes such as apical constriction in organoid cultures, with high spatiotemporal specificity[192].

Given the roles of mechanical stimuli in instructing lineage specification and morphogenesis[30,193-196], there are substantial efforts in integrating biomechanical tools that allow controls of mechanical stimuli with embryoid and organoid cultures. For cell colonies cultured on a 2D elastomeric substrate, mechanical stimuli can be introduced by changing the mechanical properties of the substrate, which are modulable through either controlling elastomer constituents[197,198] or by introducing surface microstructures such as microposts, the rigidity of which is controlled by their height and hence independent of effects on adhesive and other material surface properties[199]. To investigate the impact of exogeneous strain and stress, mechanical loading has been explicitly incorporated into in vitro cultures using bioengineering tools (**Fig. 4B**). Conventional cell or tissue straining devices generate a homogenous macroscopic strain field on a substrate or matrix through motor or pneumatic-driven displacements and thereby transmit mechanical loading to cells or tissues attached to the substrate or embedded in the matrix[200]. However, these methods often provide limited throughput and cannot model complex or heterogeneous loading dynamics. To improve throughput and facilitate mechanical screening, microfabricated platforms for both tensile and compressive loading have been developed[201-203] to investigate independent or integrative effects of loading parameters such as strain magnitude, rate and period[204]. To model the effect of shear stress, shear flow can be introduced over cell culture surfaces[205-207]. Technologies such as acoustic tweezing cytometry further enable force applications on a cellular scale without continuum strain by actuating microbubbles anchored to cell surface receptors such as integrins, and therefore decouple mechanical activation from cell deformation[208,209]. To establish a spatially patterned heterogeneous loading, inflatable PDMS microchambers are placed beneath 2D hPSC colonies at designated locations and, with increased chamber pressures, induce regional biaxial stretching of the overlying 2D hPSC colonies. This method has been applied to instruct neural[145] or mesodermal[165] lineage patterning, and can potentially be extended to stretch a 2D colony at arbitrary regions with desired shapes.

[H2] Engineering extracellular environment

Engineering properties of the extracellular environment has proved effective for inducing morphogenetic activities and therefore also provides an opportunity for investigating boundary conditions of morphogenesis (**Fig. 4C**). For cells embedded in a 3D bioengineered tissue scaffold, cell fate and morphogenesis could be mediated by matrix mechanical properties such as elasticity[16,193] and viscoelasticity[17,210]. Extracellular matrix can also be conjugated with chemical signals, such as growth factors, to create a biochemical interface for embedded tissues[211]. Furthermore, recent developments of stimulus-responsive biomaterials enable spatiotemporal control over the structural, mechanical, and biochemical cues in the extracellular matrix through light, ultrasound or

electromagnetic stimulations[212,213]. For embryoid and organoid cultures, animal-derived biological gels, such as Matrigel, have been used extensively as conductive 3D environments that facilitate spontaneous morphogenesis and lineage patterning[15,16,36-39,49,69,121,170,181,185,186,214,215]. However, the ill-defined and variable biochemical constituents in animal-derived biological gels could hinder the rationalization of morphogenetic activities manifested by embryoids and organoids in such 3D cultures[216], as is exemplified by the delicate dependence of somite-like tissue morphology on Matrigel concentration in the hPSC-based somitogenesis model[36]. To address this issue, many naturally derived and synthetic gel matrices with chemically defined components like ECM-based proteins[217] or polyethylene glycol (PEG)[218] have been developed[216,219]. More demonstrations of morphogenesis-inducing potentials of these fully defined gel matrices are required before they can be widely adopted in embryoid and organoid research.

[H1] Outlook

Stem cell-based, in vitro development models are being rapidly developed with favorable accessibility, efficiency and modulability. These in vitro development models are promising experimental tools to supplement canonical in vivo models. However, there are fundamental challenges that need to be fully addressed before in vitro development models can fully achieve their potential. The first crucial conceptual question is how to assess similarities between in vitro morphogenetic events and their in vivo counterparts. It might be difficult to expect molecular and mechanical similarities between in vitro and in vivo models at every stage of dynamic morphogenetic processes, because in vivo complexity remains to be fully understood and characterized. As a slightly lower standard, in vitro models can also be evaluated by certain critical morphogenetic phenotypes, which then requires careful scrutiny of which part of in vitro dynamics pertains to in vivo phenotypes of significance.

If the standard of in vivo relevance is clearly defined, an imminent challenge is to fully optimize the faithfulness of existing in vitro models, which can be particularly challenging if relevant in vivo knowledge is limited. To improve model fidelity, it might be necessary to increase model complexity by, for example, incorporating additional cell lineages or combining different tissues. Yet it is also important to ensure that system complexity does not overshadow the most essential morphogenetic mechanism or phenotype of interests, or negatively impact model accessibility or modulability. As one possible solution, we envision that incorporating high-precision bioengineering tools can help modularize different aspects of morphogenesis and therefore selectively target different dimensions of complexity with spatiotemporal controls. Additionally, the use of bioengineering controls can substantially improve in vitro throughput, and therefore facilitates model iteration and optimization.

Another major challenge associated with in vitro development models is how to derive mechanistic insights relevant to in vivo settings. Despite uncertainties of their applicability and predictive capacity, in vitro platforms, together with theoretical models, possess the unique potential of providing quantitative mechanistic knowledge. Animal models have been instrumental in establishing correlations between single factors, such as specific developmental genes and tissue organization. In vitro and theoretical models, conversely, allow probing combinatorial and crosstalk effects of multiple factors and thus filling the gap within in vivo derived knowledge. When combined, the quantitative power of in vitro and theoretical models can hopefully elucidate the applicable scope of observed mechanisms and phenomena, which can not only help explain contradictory experimental results but also clarify necessary conditions for normal morphogenesis. In terms of human morphogenesis and disease modeling where in vivo knowledge is limited, in vitro models might provide the most human-relevant systems to capture both the specificity and diversity among human genetic background. Nevertheless, a general research paradigm is yet to be established to organically integrate existing in vivo knowledge, in vitro models and theoretical analyses to generate systematic insights of morphogenetic principles.

In this review, we discuss about how in vivo, in vitro and theoretical models have contributed knowledge towards understanding of morphogenesis. We argue that developing in vitro and theoretical platforms opens new possibilities to improve insight into the biomechanical and biophysical principles underlying morphogenesis. With emerging stem cell technologies and bioengineering tools available for reconstituting morphogenesis in vitro, it is expected that more opportunities from in vitro and theoretical models would arise to help rationalize biological forms with new understanding that can feedback to and be integrated with in vivo knowledge.

Glossary

Lumen: a cavity or inner space enclosed by cells or tissues.

Blastocoel: A fluid-filled cavity inside pre-implantation embryos called blastocysts.

Mesenchymal-to-epithelial transition: A biological process during which loosely connected mesenchymal cells re-organize, establish apical-basal polarity and transition into an assembly of closely packed epithelial cells. Its reverse process is called epithelial-to-mesenchymal transition.

Neurulation: Formation of neural tube, which involves two different morphogenetic processes. In primary neurulation the neural plate folds inward until opposing edges come into contact, fuse, and give rise to the neural tube. In secondary neurulation, cavities form in caudal neural precursors and later merge with the neural tube formed by primary neurulation.

Epiblast: Pluripotent cells derived from inner cell mass in a blastocyst. It locates between hypoblast and trophoblast, and gives rise to three definitive germ layers.

Cleavage furrow: The indentation of a cell's surface that begins the progression of membrane separation during cell division.

Somite: Segmented, block-like structures flanking the neural tube. They are the precursors to vertebrae, part of occipital bones of the skull, skeletal muscles, dermis, cartilage, and tendons.

Rostral: Towards the head.

Caudal: Towards the tail.

Gastrulation: A morphogenetic process through which epiblast cells reorganize, differentiate, and ultimately form three spatially organized germ layers, namely (dorsal to ventral) ectoderm, mesoderm, and endoderm.

Neural tube: A tubular neural tissue and the precursor of central nervous system.

Neural plate: A region of ectoderm which contains a flat layer of columnar neuroepithelial cells.

Dorsal: Towards the back.

Medial: Towards the body midline.

Lateral: Away from the body midline.

Anencephaly: A congenital defect in the formation of neural tube, in which a baby is born without parts of the brain and skull.

Respiratory diverticulum: A ventral outpouching structure that develops from the endodermal foregut and bifurcates into left and right lung buds. Lung buds are rudiments of two lungs and the left and right primary bronchi, and the diverticulum stem forms the trachea and larynx.

Alveoli: Hollow, distensible cavities in lungs where the exchange of oxygen and carbon dioxide occurs.

Neuromesodermal progenitor: a population of bipotent progenitor cells in the caudal region of the embryo. It contributes to both spinal cord and presomitic mesoderm development.

Ventral: Towards the front.

References

1 Fu, J., Warmflash, A. & Lutolf, M. P. Stem-cell-based embryo models for fundamental research and translation. *Nat Mater* **20**, 132-144 (2021).

2 Shao, Y. & Fu, J. Engineering multiscale structural orders for high-fidelity embryoids and organoids. *Cell Stem Cell* **29**, 722-743 (2022).

3 Yin, X. *et al.* Engineering Stem Cell Organoids. *Cell Stem Cell* **18**, 25-38 (2016).

4 Brassard, J. A. & Lutolf, M. P. Engineering Stem Cell Self-organization to Build Better Organoids. *Cell Stem Cell* **24**, 860-876 (2019).

5 Torres-Sanchez, A., Kerr Winter, M. & Salbreux, G. Tissue hydraulics: Physics of lumen formation and interaction. *Cells Dev* **168**, 203724 (2021).

6 Dumortier, J. G. *et al.* Hydraulic fracturing and active coarsening position the lumen of the mouse blastocyst. *Science* **365**, 465-468 (2019).

7 Harrington, M. J., Hong, E. & Brewster, R. Comparative analysis of neurulation: first impressions do not count. *Molecular Reproduction and Development: Incorporating Gamete Research* **76**, 954-965 (2009).

8 Bedzhov, I. & Zernicka-Goetz, M. Self-organizing properties of mouse pluripotent cells initiate morphogenesis upon implantation. *Cell* **156**, 1032-1044 (2014).

9 Kim, Y. S. *et al.* Deciphering epiblast lumenogenesis reveals proamniotic cavity control of embryo growth and patterning. *Sci Adv* **7** (2021).

10 Molè, M. A. *et al.* Integrin β1 coordinates survival and morphogenesis of the embryonic lineage upon implantation and pluripotency transition. *Cell Reports* **34**, 108834 (2021).

11 Orietti, L. C. *et al.* Embryo size regulates the timing and mechanism of pluripotent tissue morphogenesis. *Stem Cell Reports* **16**, 1182-1196 (2021).

12 Taniguchi, K. *et al.* Lumen formation is an intrinsic property of isolated human pluripotent stem cells. *Stem Cell Reports* **5**, 954-962 (2015).

13 Taniguchi, K. *et al.* An apicosome initiates self-organizing morphogenesis of human pluripotent stem cells. *J Cell Biol* **216**, 3981-3990 (2017).

14 Wang, S. *et al.* Spatially resolved cell polarity proteomics of a human epiblast model. *Sci Adv* **7** (2021).

15 Shao, Y. *et al.* A pluripotent stem cell-based model for post-implantation human amniotic sac development. *Nat Commun* **8**, 208 (2017).

16 Shao, Y. *et al.* Self-organized amniogenesis by human pluripotent stem cells in a biomimetic implantation-like niche. *Nat Mater* **16**, 419-425 (2017).

17 Indana, D., Agarwal, P., Bhutani, N. & Chaudhuri, O. Viscoelasticity and Adhesion Signaling in Biomaterials Control Human Pluripotent Stem Cell Morphogenesis in 3D Culture. *Adv Mater* **33**, e2101966 (2021).

18 Dasgupta, S., Gupta, K., Zhang, Y., Viasnoff, V. & Prost, J. Physics of lumen growth. *Proc Natl Acad Sci U S A* **115**, E4751-E4757 (2018).

19 Dokmegang, J., Yap, M. H., Han, L., Cavaliere, M. & Doursat, R. Computational modelling unveils how epiblast remodelling and positioning rely on trophectoderm morphogenesis during mouse implantation. *Plos one* **16**, e0254763 (2021).

20 Burgess, R., Rawls, A., Brown, D., Bradley, A. & Olson, E. N. Requirement of the paraxis gene for somite formation and musculoskeletal patterning. *Nature* **384**, 570-573 (1996).

21 Rowton, M. *et al.* Regulation of mesenchymal-to-epithelial transition by PARAXIS during somitogenesis. *Dev Dyn* **242**, 1332-1344 (2013).

22 Wiggan, O., Fadel, M. P. & Hamel, P. A. Pax3 induces cell aggregation and regulates phenotypic mesenchymal-epithelial interconversion. *J Cell Sci* **115**, 517-529 (2002).

23 Nakaya, Y., Kuroda, S., Katagiri, Y. T., Kaibuchi, K. & Takahashi, Y. Mesenchymal-epithelial transition during somitic segmentation is regulated by differential roles of Cdc42 and Rac1. *Developmental cell* **7**, 425-438 (2004).

24 Takahashi, Y., Sato, Y., Suetsugu, R. & Nakaya, Y. Mesenchymal-to-epithelial transition during somitic segmentation: a novel approach to studying the roles of Rho family GTPases in morphogenesis. *Cells Tissues Organs* **179**, 36-42 (2005).
25 Kulesa, P. M. & Fraser, S. E. Cell dynamics during somite boundary formation revealed by time-lapse analysis. *Science* **298**, 991-995 (2002).
26 Cooke, J. & Zeeman, E. C. A clock and wavefront model for control of the number of repeated structures during animal morphogenesis. *J Theor Biol* **58**, 455-476 (1976).
27 Dubrulle, J., McGrew, M. J. & Pourquié, O. FGF signaling controls somite boundary position and regulates segmentation clock control of spatiotemporal Hox gene activation. *Cell* **106**, 219-232 (2001).
28 Dubrulle, J. & Pourquie, O. From head to tail: links between the segmentation clock and antero-posterior patterning of the embryo. *Curr Opin Genet Dev* **12**, 519-523 (2002).
29 Simsek, M. F. *et al.* Periodic inhibition of Erk activity drives sequential somite segmentation. *Nature* **613**, 153-159 (2023).
30 Nelemans, B. K. A., Schmitz, M., Tahir, H., Merks, R. M. H. & Smit, T. H. Somite Division and New Boundary Formation by Mechanical Strain. *iScience* **23**, 100976 (2020).
31 Naganathan, S. R., Popovic, M. & Oates, A. C. Left-right symmetry of zebrafish embryos requires somite surface tension. *Nature* **605**, 516-521 (2022).
32 Richardson, M. K., Allen, S. P., Wright, G. M., Raynaud, A. & Hanken, J. Somite number and vertebrate evolution. *Development* **125**, 151-160 (1998).
33 Gomez, C. *et al.* Control of segment number in vertebrate embryos. *Nature* **454**, 335-339 (2008).
34 Eckalbar, W. L., Fisher, R. E., Rawls, A. & Kusumi, K. Scoliosis and segmentation defects of the vertebrae. *Wiley Interdiscip Rev Dev Biol* **1**, 401-423 (2012).
35 Budjan, C. *et al.* Paraxial mesoderm organoids model development of human somites. *Elife* **11** (2022).
36 Sanaki-Matsumiya, M. *et al.* Periodic formation of epithelial somites from human pluripotent stem cells. *Nat Commun* **13**, 2325 (2022).
37 Miao, Y. *et al.* Reconstruction and deconstruction of human somitogenesis in vitro. *Nature* (2022).
38 Yamanaka, Y. *et al.* Reconstituting human somitogenesis in vitro. *Nature* (2022).
39 Yaman, Y. I. & Ramanathan, S. Controlling human organoid symmetry breaking reveals signaling gradients drive segmentation clock waves. *Cell* (2023).
40 Morelli, L. G. *et al.* Delayed coupling theory of vertebrate segmentation. *HFSP J* **3**, 55-66 (2009).
41 Hubaud, A., Regev, I., Mahadevan, L. & Pourquie, O. Excitable Dynamics and Yap-Dependent Mechanical Cues Drive the Segmentation Clock. *Cell* **171**, 668-682 e611 (2017).
42 Baker, R. E., Schnell, S. & Maini, P. K. A clock and wavefront mechanism for somite formation. *Dev Biol* **293**, 116-126 (2006).
43 Hester, S. D., Belmonte, J. M., Gens, J. S., Clendenon, S. G. & Glazier, J. A. A multi-cell, multi-scale model of vertebrate segmentation and somite formation. *PLoS Comput Biol* **7**, e1002155 (2011).
44 Adhyapok, P. *et al.* A mechanical model of early somite segmentation. *iScience* **24**, 102317 (2021).
45 Nikolopoulou, E., Galea, G. L., Rolo, A., Greene, N. D. & Copp, A. J. Neural tube closure: cellular, molecular and biomechanical mechanisms. *Development* **144**, 552-566 (2017).
46 Morriss-Kay, G. M. Growth and development of pattern in the cranial neural epithelium of rat embryos during neurulation. *J Embryol Exp Morphol* **65 Suppl**, 225-241 (1981).
47 Sawyer, J. M. *et al.* Apical constriction: a cell shape change that can drive morphogenesis. *Developmental biology* **341**, 5-19 (2010).
48 Botto, L. D., Moore, C. A., Khoury, M. J. & Erickson, J. D. Neural-tube defects. *New England journal of medicine* **341**, 1509-1519 (1999).

49 Karzbrun, E. *et al.* Human neural tube morphogenesis in vitro by geometric constraints. *Nature* **599**, 268-272 (2021).
50 Sahni, G. *et al.* A Micropatterned Human-Specific Neuroepithelial Tissue for Modeling Gene and Drug-Induced Neurodevelopmental Defects. *Adv Sci (Weinh)* **8**, e2101786 (2021).
51 Jacobson, A. G. & Gordon, R. Changes in the shape of the developing vertebrate nervous system analyzed experimentally, mathematically and by computer simulation. *J Exp Zool* **197**, 191-246 (1976).
52 Odell, G. M., Oster, G., Alberch, P. & Burnside, B. The mechanical basis of morphogenesis: I. Epithelial folding and invagination. *Developmental biology* **85**, 446-462 (1981).
53 Inoue, Y. *et al.* Mechanical roles of apical constriction, cell elongation, and cell migration during neural tube formation in Xenopus. *Biomech Model Mechanobiol* **15**, 1733-1746 (2016).
54 Fletcher, A. G., Osterfield, M., Baker, R. E. & Shvartsman, S. Y. Vertex models of epithelial morphogenesis. *Biophys J* **106**, 2291-2304 (2014).
55 de Goederen, V., Vetter, R., McDole, K. & Iber, D. Hinge point emergence in mammalian spinal neurulation. *Proceedings of the National Academy of Sciences* **119**, e2117075119 (2022).
56 Chen, X. & Brodland, G. W. Multi-scale finite element modeling allows the mechanics of amphibian neurulation to be elucidated. *Physical Biology* **5**, 015003 (2008).
57 Taber, L. A. Biomechanics of growth, remodeling, and morphogenesis. (1995).
58 Brodland, G. W., Chen, X., Lee, P. & Marsden, M. From genes to neural tube defects (NTDs): insights from multiscale computational modeling. *HFSP J* **4**, 142-152 (2010).
59 Helander, H. F. & Fandriks, L. Surface area of the digestive tract - revisited. *Scand J Gastroenterol* **49**, 681-689 (2014).
60 Shyer, A. E. *et al.* Villification: how the gut gets its villi. *Science* **342**, 212-218 (2013).
61 Shyer, A. E., Huycke, T. R., Lee, C., Mahadevan, L. & Tabin, C. J. Bending gradients: how the intestinal stem cell gets its home. *Cell* **161**, 569-580 (2015).
62 Walton, K. D. *et al.* Villification in the mouse: Bmp signals control intestinal villus patterning. *Development* **143**, 427-436 (2016).
63 Mao, J., Kim, B. M., Rajurkar, M., Shivdasani, R. A. & McMahon, A. P. Hedgehog signaling controls mesenchymal growth in the developing mammalian digestive tract. *Development* **137**, 1721-1729 (2010).
64 Rao-Bhatia, A. *et al.* Hedgehog-Activated Fat4 and PCP Pathways Mediate Mesenchymal Cell Clustering and Villus Formation in Gut Development. *Dev Cell* **52**, 647-658 e646 (2020).
65 Karlsson, L., Lindahl, P., Heath, J. K. & Betsholtz, C. Abnormal gastrointestinal development in PDGF-A and PDGFR-(alpha) deficient mice implicates a novel mesenchymal structure with putative instructive properties in villus morphogenesis. *Development* **127**, 3457-3466 (2000).
66 Chin, A. M., Hill, D. R., Aurora, M. & Spence, J. R. Morphogenesis and maturation of the embryonic and postnatal intestine. *Semin Cell Dev Biol* **66**, 81-93 (2017).
67 Walton, K. D., Freddo, A. M., Wang, S. & Gumucio, D. L. Generation of intestinal surface: an absorbing tale. *Development* **143**, 2261-2272 (2016).
68 Sumigray, K. D., Terwilliger, M. & Lechler, T. Morphogenesis and Compartmentalization of the Intestinal Crypt. *Dev Cell* **45**, 183-197 e185 (2018).
69 Spence, J. R. *et al.* Directed differentiation of human pluripotent stem cells into intestinal tissue in vitro. *Nature* **470**, 105-109 (2011).
70 Mithal, A. *et al.* Generation of mesenchyme free intestinal organoids from human induced pluripotent stem cells. *Nat Commun* **11**, 215 (2020).
71 Workman, M. J. *et al.* Engineered human pluripotent-stem-cell-derived intestinal tissues with a functional enteric nervous system. *Nat Med* **23**, 49-59 (2017).
72 Yang, Q. *et al.* Cell fate coordinates mechano-osmotic forces in intestinal crypt formation. *Nat Cell Biol* **23**, 733-744 (2021).
73 Perez-Gonzalez, C. *et al.* Mechanical compartmentalization of the intestinal organoid enables crypt folding and collective cell migration. *Nat Cell Biol* **23**, 745-757 (2021).

74 Hartl, L., Huelsz-Prince, G., van Zon, J. & Tans, S. J. Apical constriction is necessary for crypt formation in small intestinal organoids. *Developmental biology* **450**, 76-81 (2019).
75 Serra, D. *et al.* Self-organization and symmetry breaking in intestinal organoid development. *Nature* **569**, 66-72 (2019).
76 Krndija, D. *et al.* Active cell migration is critical for steady-state epithelial turnover in the gut. *Science* **365**, 705-710 (2019).
77 Sato, T. *et al.* Single Lgr5 stem cells build crypt-villus structures in vitro without a mesenchymal niche. *Nature* **459**, 262-265 (2009).
78 Balbi, V. & Ciarletta, P. Morpho-elasticity of intestinal villi. *Journal of the Royal Society Interface* **10**, 20130109 (2013).
79 Hannezo, E., Prost, J. & Joanny, J.-F. Instabilities of monolayered epithelia: shape and structure of villi and crypts. *Physical Review Letters* **107**, 078104 (2011).
80 Ben Amar, M. & Jia, F. Anisotropic growth shapes intestinal tissues during embryogenesis. *Proc Natl Acad Sci U S A* **110**, 10525-10530 (2013).
81 Freddo, A. M. *et al.* Coordination of signaling and tissue mechanics during morphogenesis of murine intestinal villi: a role for mitotic cell rounding. *Integr Biol (Camb)* **8**, 918-928 (2016).
82 Thalheim, T. *et al.* Stem cell competition in the gut: insights from multi-scale computational modelling. *J R Soc Interface* **13** (2016).
83 Buske, P. *et al.* On the biomechanics of stem cell niche formation in the gut--modelling growing organoids. *FEBS J* **279**, 3475-3487 (2012).
84 Itzkovitz, S., Blat, I. C., Jacks, T., Clevers, H. & van Oudenaarden, A. Optimality in the development of intestinal crypts. *Cell* **148**, 608-619 (2012).
85 Almet, A. A., Maini, P. K., Moulton, D. E. & Byrne, H. M. Modeling perspectives on the intestinal crypt, a canonical system for growth, mechanics, and remodeling. *Current Opinion in Biomedical Engineering* **15**, 32-39 (2020).
86 Schoenwolf, G. C., Bleyl, S. B., Brauer, P. R. & Francis-West, P. H. *Larsen's human embryology*. (Elsevier Health Sciences, 2014).
87 Metzger, R. J., Klein, O. D., Martin, G. R. & Krasnow, M. A. The branching programme of mouse lung development. *Nature* **453**, 745-750 (2008).
88 Swarr, D. T. & Morrisey, E. E. Lung endoderm morphogenesis: gasping for form and function. *Annu Rev Cell Dev Biol* **31**, 553-573 (2015).
89 Whitsett, J. A., Kalin, T. V., Xu, Y. & Kalinichenko, V. V. Building and Regenerating the Lung Cell by Cell. *Physiol Rev* **99**, 513-554 (2019).
90 Goodwin, K. & Nelson, C. M. Branching morphogenesis. *Development* **147** (2020).
91 Lang, C., Conrad, L. & Iber, D. Organ-Specific Branching Morphogenesis. *Front Cell Dev Biol* **9**, 671402 (2021).
92 Varner, V. D. & Nelson, C. M. Cellular and physical mechanisms of branching morphogenesis. *Development* **141**, 2750-2759 (2014).
93 Goodwin, K. *et al.* Smooth muscle differentiation shapes domain branches during mouse lung development. *Development* **146** (2019).
94 Kim, H. Y. *et al.* Localized smooth muscle differentiation is essential for epithelial bifurcation during branching morphogenesis of the mammalian lung. *Developmental Cell* **34**, 719-726 (2015).
95 Bellusci, S., Grindley, J., Emoto, H., Itoh, N. & Hogan, B. L. Fibroblast growth factor 10 (FGF10) and branching morphogenesis in the embryonic mouse lung. *Development* **124**, 4867-4878 (1997).
96 Volckaert, T. *et al.* Localized Fgf10 expression is not required for lung branching morphogenesis but prevents differentiation of epithelial progenitors. *Development* **140**, 3731-3742 (2013).
97 Chen, Y. W. *et al.* A three-dimensional model of human lung development and disease from pluripotent stem cells. *Nat Cell Biol* **19**, 542-549 (2017).

98 Miller, A. J. *et al.* In Vitro Induction and In Vivo Engraftment of Lung Bud Tip Progenitor Cells Derived from Human Pluripotent Stem Cells. *Stem Cell Reports* **10**, 101-119 (2018).
99 Strikoudis, A. *et al.* Modeling of Fibrotic Lung Disease Using 3D Organoids Derived from Human Pluripotent Stem Cells. *Cell Rep* **27**, 3709-3723 e3705 (2019).
100 Tian, L. *et al.* Human pluripotent stem cell-derived lung organoids: Potential applications in development and disease modeling. *Wiley Interdiscip Rev Dev Biol* **10**, e399 (2021).
101 Dye, B. R. *et al.* In vitro generation of human pluripotent stem cell derived lung organoids. *Elife* **4** (2015).
102 McCauley, K. B. *et al.* Efficient Derivation of Functional Human Airway Epithelium from Pluripotent Stem Cells via Temporal Regulation of Wnt Signaling. *Cell Stem Cell* **20**, 844-857 e846 (2017).
103 Konishi, S. *et al.* Directed Induction of Functional Multi-ciliated Cells in Proximal Airway Epithelial Spheroids from Human Pluripotent Stem Cells. *Stem Cell Reports* **6**, 18-25 (2016).
104 Menshykau, D., Blanc, P., Unal, E., Sapin, V. & Iber, D. An interplay of geometry and signaling enables robust lung branching morphogenesis. *Development* **141**, 4526-4536 (2014).
105 Menshykau, D., Kraemer, C. & Iber, D. Branch mode selection during early lung development. *PLoS Comput Biol* **8**, e1002377 (2012).
106 Varner, V. D., Gleghorn, J. P., Miller, E., Radisky, D. C. & Nelson, C. M. Mechanically patterning the embryonic airway epithelium. *Proc Natl Acad Sci U S A* **112**, 9230-9235 (2015).
107 Hannezo, E. *et al.* A Unifying Theory of Branching Morphogenesis. *Cell* **171**, 242-255 e227 (2017).
108 Benazeraf, B. & Pourquie, O. Formation and segmentation of the vertebrate body axis. *Annu Rev Cell Dev Biol* **29**, 1-26 (2013).
109 Takada, S. *et al.* Wnt-3a regulates somite and tailbud formation in the mouse embryo. *Genes Dev* **8**, 174-189 (1994).
110 Bertrand, N., Medevielle, F. & Pituello, F. FGF signalling controls the timing of Pax6 activation in the neural tube. *Development* **127**, 4837-4843 (2000).
111 Gouti, M. *et al.* A Gene Regulatory Network Balances Neural and Mesoderm Specification during Vertebrate Trunk Development. *Dev Cell* **41**, 243-261 e247 (2017).
112 Koch, F. *et al.* Antagonistic Activities of Sox2 and Brachyury Control the Fate Choice of Neuro-Mesodermal Progenitors. *Dev Cell* **42**, 514-526 e517 (2017).
113 Olivera-Martinez, I., Harada, H., Halley, P. A. & Storey, K. G. Loss of FGF-dependent mesoderm identity and rise of endogenous retinoid signalling determine cessation of body axis elongation. *PLoS Biol* **10**, e1001415 (2012).
114 Boulet, A. M. & Capecchi, M. R. Signaling by FGF4 and FGF8 is required for axial elongation of the mouse embryo. *Developmental biology* **371**, 235-245 (2012).
115 Benazeraf, B. *et al.* A random cell motility gradient downstream of FGF controls elongation of an amniote embryo. *Nature* **466**, 248-252 (2010).
116 Mongera, A. *et al.* A fluid-to-solid jamming transition underlies vertebrate body axis elongation. *Nature* **561**, 401-405 (2018).
117 Xiong, F., Ma, W., Benazeraf, B., Mahadevan, L. & Pourquie, O. Mechanical Coupling Coordinates the Co-elongation of Axial and Paraxial Tissues in Avian Embryos. *Dev Cell* **55**, 354-366 e355 (2020).
118 Beccari, L. *et al.* Multi-axial self-organization properties of mouse embryonic stem cells into gastruloids. *Nature* **562**, 272-276 (2018).
119 van den Brink, S. C. *et al.* Single-cell and spatial transcriptomics reveal somitogenesis in gastruloids. *Nature* **582**, 405-409 (2020).
120 Moris, N. *et al.* An in vitro model of early anteroposterior organization during human development. *Nature* **582**, 410-415 (2020).
121 Veenvliet, J. V. *et al.* Mouse embryonic stem cells self-organize into trunk-like structures with neural tube and somites. *Science* **370**, eaba4937 (2020).

122 Anand, G. M. *et al.* Controlling organoid symmetry breaking uncovers an excitable system underlying human axial elongation. *Cell* **186**, 497-512 e423 (2023).
123 Libby, A. R. G. *et al.* Axial elongation of caudalized human organoids mimics aspects of neural tube development. *Development* **148** (2021).
124 Pennimpede, T. *et al.* In vivo knockdown of Brachyury results in skeletal defects and urorectal malformations resembling caudal regression syndrome. *Dev Biol* **372**, 55-67 (2012).
125 Amin, S. *et al.* Cdx and T Brachyury Co-activate Growth Signaling in the Embryonic Axial Progenitor Niche. *Cell Rep* **17**, 3165-3177 (2016).
126 Regev, I., Guevorkian, K., Gupta, A., Pourquié, O. & Mahadevan, L. Rectified random cell motility as a mechanism for embryo elongation. *Development* **149**, dev199423 (2022).
127 Lawton, A. K. *et al.* Regulated tissue fluidity steers zebrafish body elongation. *Development* **140**, 573-582 (2013).
128 Valet, M., Siggia, E. D. & Brivanlou, A. H. Mechanical regulation of early vertebrate embryogenesis. *Nat Rev Mol Cell Biol* **23**, 169-184 (2022).
129 Turing, A. M. The chemical basis of morphogenesis. 1953. *Bull Math Biol* **52**, 153-197; discussion 119-152 (1990).
130 Kondo, S. & Miura, T. Reaction-diffusion model as a framework for understanding biological pattern formation. *science* **329**, 1616-1620 (2010).
131 Howard, J., Grill, S. W. & Bois, J. S. Turing's next steps: the mechanochemical basis of morphogenesis. *Nat Rev Mol Cell Biol* **12**, 392-398 (2011).
132 Almuedo-Castillo, M. *et al.* Scale-invariant patterning by size-dependent inhibition of Nodal signalling. *Nat Cell Biol* **20**, 1032-1042 (2018).
133 Werner, S. *et al.* Scaling and regeneration of self-organized patterns. *Phys Rev Lett* **114**, 138101 (2015).
134 Recho, P., Hallou, A. & Hannezo, E. Theory of mechanochemical patterning in biphasic biological tissues. *Proc Natl Acad Sci U S A* **116**, 5344-5349 (2019).
135 Meinhardt, H. *The algorithmic beauty of sea shells*. (Springer Science & Business Media, 2009).
136 Watanabe, M. & Kondo, S. Is pigment patterning in fish skin determined by the Turing mechanism? *Trends in Genetics* **31**, 88-96 (2015).
137 Glover, J. D. *et al.* The developmental basis of fingerprint pattern formation and variation. *Cell*.
138 Iber, D. & Menshykau, D. The control of branching morphogenesis. *Open Biol* **3**, 130088 (2013).
139 Zhang, Z., Zwick, S., Loew, E., Grimley, J. S. & Ramanathan, S. Mouse embryo geometry drives formation of robust signaling gradients through receptor localization. *Nature communications* **10**, 4516 (2019).
140 Gao, H., Ji, B., Jäger, I. L., Arzt, E. & Fratzl, P. Materials become insensitive to flaws at nanoscale: lessons from nature. *Proceedings of the national Academy of Sciences* **100**, 5597-5600 (2003).
141 Savin, T. *et al.* On the growth and form of the gut. *Nature* **476**, 57-62 (2011).
142 Bauwens, C. L. *et al.* Control of human embryonic stem cell colony and aggregate size heterogeneity influences differentiation trajectories. *Stem Cells* **26**, 2300-2310 (2008).
143 Tewary, M. *et al.* A stepwise model of reaction-diffusion and positional information governs self-organized human peri-gastrulation-like patterning. *Development* **144**, 4298-4312 (2017).
144 Etoc, F. *et al.* A balance between secreted inhibitors and edge sensing controls gastruloid self-organization. *Developmental cell* **39**, 302-315 (2016).
145 Xue, X. *et al.* Mechanics-guided embryonic patterning of neuroectoderm tissue from human pluripotent stem cells. *Nat Mater* **17**, 633-641 (2018).
146 Diaz-Cuadros, M. *et al.* Metabolic regulation of species-specific developmental rates. *Nature* **613**, 550-557 (2023).
147 Lazaro, J. *et al.* A stem cell zoo uncovers intracellular scaling of developmental tempo across mammals. *bioRxiv*, 2022.2010. 2013.512072 (2022).

148 Matsuda, M. *et al.* Species-specific segmentation clock periods are due to differential biochemical reaction speeds. *Science* **369**, 1450-1455 (2020).
149 Matsuda, M. *et al.* Recapitulating the human segmentation clock with pluripotent stem cells. *Nature* **580**, 124-129 (2020).
150 Diaz-Cuadros, M. *et al.* In vitro characterization of the human segmentation clock. *Nature* **580**, 113-118 (2020).
151 Rogers, K. W. & Schier, A. F. Morphogen gradients: from generation to interpretation. *Annu Rev Cell Dev Biol* **27**, 377-407 (2011).
152 Stapornwongkul, K. S. & Vincent, J. P. Generation of extracellular morphogen gradients: the case for diffusion. *Nat Rev Genet* **22**, 393-411 (2021).
153 Wolpert, L. Positional information and the spatial pattern of cellular differentiation. *J Theor Biol* **25**, 1-47 (1969).
154 Nordstrom, U., Jessell, T. M. & Edlund, T. Progressive induction of caudal neural character by graded Wnt signaling. *Nat Neurosci* **5**, 525-532 (2002).
155 Swindell, E. C. *et al.* Complementary domains of retinoic acid production and degradation in the early chick embryo. *Dev Biol* **216**, 282-296 (1999).
156 Duester, G. Retinoic acid synthesis and signaling during early organogenesis. *Cell* **134**, 921-931 (2008).
157 Towers, M. & Tickle, C. Growing models of vertebrate limb development. *Development* **136**, 179-190 (2009).
158 Tickle, C., Summerbell, D. & Wolpert, L. Positional signalling and specification of digits in chick limb morphogenesis. *Nature* **254**, 199-202 (1975).
159 Barriga, E. H., Franze, K., Charras, G. & Mayor, R. Tissue stiffening coordinates morphogenesis by triggering collective cell migration in vivo. *Nature* **554**, 523-527 (2018).
160 Zhu, M. *et al.* Spatial mapping of tissue properties in vivo reveals a 3D stiffness gradient in the mouse limb bud. *Proc Natl Acad Sci U S A* **117**, 4781-4791 (2020).
161 Shellard, A. & Mayor, R. Collective durotaxis along a self-generated stiffness gradient in vivo. *Nature* **600**, 690-694 (2021).
162 Zheng, Y. *et al.* Controlled modelling of human epiblast and amnion development using stem cells. *Nature* **573**, 421-425 (2019).
163 Manfrin, A. *et al.* Engineered signaling centers for the spatially controlled patterning of human pluripotent stem cells. *Nat Methods* **16**, 640-648 (2019).
164 Rifes, P. *et al.* Modeling neural tube development by differentiation of human embryonic stem cells in a microfluidic WNT gradient. *Nat Biotechnol* **38**, 1265-1273 (2020).
165 Muncie, J. M. *et al.* Mechanical Tension Promotes Formation of Gastrulation-like Nodes and Patterns Mesoderm Specification in Human Embryonic Stem Cells. *Dev Cell* **55**, 679-694 e611 (2020).
166 Saadaoui, M., Rocancourt, D., Roussel, J., Corson, F. & Gros, J. A tensile ring drives tissue flows to shape the gastrulating amniote embryo. *Science* **367**, 453-458 (2020).
167 Liu, X. *et al.* Modelling human blastocysts by reprogramming fibroblasts into iBlastoids. *Nature* **591**, 627-632 (2021).
168 Yu, L. *et al.* Blastocyst-like structures generated from human pluripotent stem cells. *Nature* **591**, 620-626 (2021).
169 Kagawa, H. *et al.* Human blastoids model blastocyst development and implantation. *Nature* **601**, 600-605 (2022).
170 Zheng, Y. *et al.* Dorsal-ventral patterned neural cyst from human pluripotent stem cells in a neurogenic niche. *Sci Adv* **5**, eaax5933 (2019).
171 Harrison, S. E., Sozen, B., Christodoulou, N., Kyprianou, C. & Zernicka-Goetz, M. Assembly of embryonic and extraembryonic stem cells to mimic embryogenesis in vitro. *Science* **356** (2017).
172 Whitesides, G. M., Ostuni, E., Takayama, S., Jiang, X. & Ingber, D. E. Soft lithography in biology and biochemistry. *Annual review of biomedical engineering* **3**, 335-373 (2001).

173 Xia, Y. & Whitesides, G. M. Soft lithography. *Annual review of materials science* **28**, 153-184 (1998).
174 Warmflash, A., Sorre, B., Etoc, F., Siggia, E. D. & Brivanlou, A. H. A method to recapitulate early embryonic spatial patterning in human embryonic stem cells. *Nat Methods* **11**, 847-854 (2014).
175 Kilian, K. A., Bugarija, B., Lahn, B. T. & Mrksich, M. Geometric cues for directing the differentiation of mesenchymal stem cells. *Proc Natl Acad Sci U S A* **107**, 4872-4877 (2010).
176 Alom Ruiz, S. & Chen, C. S. Microcontact printing: A tool to pattern. *Soft Matter* **3**, 168-177 (2007).
177 Bernard, A., Renault, J. P., Michel, B., Bosshard, H. R. & Delamarche, E. Microcontact printing of proteins. *Advanced Materials* **12**, 1067-1070 (2000).
178 Karp, J. M. *et al.* Controlling size, shape and homogeneity of embryoid bodies using poly(ethylene glycol) microwells. *Lab Chip* **7**, 786-794 (2007).
179 Nelson, C. M., Vanduijn, M. M., Inman, J. L., Fletcher, D. A. & Bissell, M. J. Tissue geometry determines sites of mammary branching morphogenesis in organotypic cultures. *Science* **314**, 298-300 (2006).
180 Dahlmann, J. *et al.* The use of agarose microwells for scalable embryoid body formation and cardiac differentiation of human and murine pluripotent stem cells. *Biomaterials* **34**, 2463-2471 (2013).
181 Chen, K. *et al.* Branching development of early post-implantation human embryonic-like tissues in 3D stem cell culture. *Biomaterials* **275**, 120898 (2021).
182 Ma, Z. *et al.* Self-organizing human cardiac microchambers mediated by geometric confinement. *Nat Commun* **6**, 7413 (2015).
183 Gjorevski, N. *et al.* Tissue geometry drives deterministic organoid patterning. *Science* **375**, eaaw9021 (2022).
184 Nelson, C. M., Inman, J. L. & Bissell, M. J. Three-dimensional lithographically defined organotypic tissue arrays for quantitative analysis of morphogenesis and neoplastic progression. *Nat Protoc* **3**, 674-678 (2008).
185 Nikolaev, M. *et al.* Homeostatic mini-intestines through scaffold-guided organoid morphogenesis. *Nature* **585**, 574-578 (2020).
186 Brassard, J. A., Nikolaev, M., Hübscher, T., Hofer, M. & Lutolf, M. P. Recapitulating macro-scale tissue self-organization through organoid bioprinting. *Nature Materials* **20**, 22-29 (2021).
187 Bratt-Leal, A. M., Nguyen, A. H., Hammersmith, K. A., Singh, A. & McDevitt, T. C. A microparticle approach to morphogen delivery within pluripotent stem cell aggregates. *Biomaterials* **34**, 7227-7235 (2013).
188 Suri, S. *et al.* Microfluidic-based patterning of embryonic stem cells for in vitro development studies. *Lab Chip* **13**, 4617-4624 (2013).
189 O'Grady, B. *et al.* Spatiotemporal control and modeling of morphogen delivery to induce gradient patterning of stem cell differentiation using fluidic channels. *Biomater Sci* **7**, 1358-1371 (2019).
190 Demers, C. J. *et al.* Development-on-chip: in vitro neural tube patterning with a microfluidic device. *Development* **143**, 1884-1892 (2016).
191 Samal, P., van Blitterswijk, C., Truckenmüller, R. & Giselbrecht, S. Grow with the flow: when morphogenesis meets microfluidics. *Advanced Materials* **31**, 1805764 (2019).
192 Martinez-Ara, G. *et al.* Optogenetic control of apical constriction induces synthetic morphogenesis in mammalian tissues. *Nat Commun* **13**, 5400 (2022).
193 Engler, A. J., Sen, S., Sweeney, H. L. & Discher, D. E. Matrix elasticity directs stem cell lineage specification. *Cell* **126**, 677-689 (2006).
194 Vining, K. H. & Mooney, D. J. Mechanical forces direct stem cell behaviour in development and regeneration. *Nat Rev Mol Cell Biol* **18**, 728-742 (2017).
195 Abdel Fattah, A. R. *et al.* Actuation enhances patterning in human neural tube organoids. *Nat Commun* **12**, 3192 (2021).

196 Li, Y. *et al.* Volumetric Compression Induces Intracellular Crowding to Control Intestinal Organoid Growth via Wnt/beta-Catenin Signaling. *Cell Stem Cell* **28**, 63-78 e67 (2021).
197 Pelham, R. J., Jr. & Wang, Y. Cell locomotion and focal adhesions are regulated by substrate flexibility. *Proc Natl Acad Sci U S A* **94**, 13661-13665 (1997).
198 Sun, Y. *et al.* Hippo/YAP-mediated rigidity-dependent motor neuron differentiation of human pluripotent stem cells. *Nat Mater* **13**, 599-604 (2014).
199 Fu, J. *et al.* Mechanical regulation of cell function with geometrically modulated elastomeric substrates. *Nat Methods* **7**, 733-736 (2010).
200 Riehl, B. D., Park, J. H., Kwon, I. K. & Lim, J. Y. Mechanical stretching for tissue engineering: two-dimensional and three-dimensional constructs. *Tissue Eng Part B Rev* **18**, 288-300 (2012).
201 Moraes, C., Wang, G., Sun, Y. & Simmons, C. A. A microfabricated platform for high-throughput unconfined compression of micropatterned biomaterial arrays. *Biomaterials* **31**, 577-584 (2010).
202 Sakthivel, K. *et al.* High Throughput Screening of Cell Mechanical Response Using a Stretchable 3D Cellular Microarray Platform. *Small* **16**, e2000941 (2020).
203 Hsieh, H. Y. *et al.* Gradient static-strain stimulation in a microfluidic chip for 3D cellular alignment. *Lab Chip* **14**, 482-493 (2014).
204 Liu, H., Usprech, J. F., Parameshwar, P. K., Sun, Y. & Simmons, C. A. Combinatorial screen of dynamic mechanical stimuli for predictive control of MSC mechano-responsiveness. *Sci Adv* **7** (2021).
205 Shemesh, J. *et al.* Flow-induced stress on adherent cells in microfluidic devices. *Lab Chip* **15**, 4114-4127 (2015).
206 Yu, W. *et al.* A microfluidic-based multi-shear device for investigating the effects of low fluid-induced stresses on osteoblasts. *PLoS One* **9**, e89966 (2014).
207 Mandrycky, C., Hadland, B. & Zheng, Y. 3D curvature-instructed endothelial flow response and tissue vascularization. *Sci Adv* **6** (2020).
208 Topal, T. *et al.* Acoustic Tweezing Cytometry Induces Rapid Initiation of Human Embryonic Stem Cell Differentiation. *Sci Rep* **8**, 12977 (2018).
209 Chen, D. *et al.* Two-bubble acoustic tweezing cytometry for biomechanical probing and stimulation of cells. *Biophys J* **108**, 32-42 (2015).
210 Chaudhuri, O. *et al.* Hydrogels with tunable stress relaxation regulate stem cell fate and activity. *Nat Mater* **15**, 326-334 (2016).
211 Mitchell, A. C., Briquez, P. S., Hubbell, J. A. & Cochran, J. R. Engineering growth factors for regenerative medicine applications. *Acta Biomater* **30**, 1-12 (2016).
212 Gelmi, A. & Schutt, C. E. Stimuli-Responsive Biomaterials: Scaffolds for Stem Cell Control. *Adv Healthc Mater* **10**, e2001125 (2021).
213 Yavitt, F. M. *et al.* In situ modulation of intestinal organoid epithelial curvature through photoinduced viscoelasticity directs crypt morphogenesis. *Science Advances* **9**, eadd5668 (2023).
214 van den Brink, S. C. *et al.* Single-cell and spatial transcriptomics reveal somitogenesis in gastruloids. *Nature* **582**, 405-409 (2020).
215 Drakhlis, L. *et al.* Human heart-forming organoids recapitulate early heart and foregut development. *Nat Biotechnol* **39**, 737-746 (2021).
216 Aisenbrey, E. A. & Murphy, W. L. Synthetic alternatives to Matrigel. *Nat Rev Mater* **5**, 539-551 (2020).
217 Flaim, C. J., Chien, S. & Bhatia, S. N. An extracellular matrix microarray for probing cellular differentiation. *Nat Methods* **2**, 119-125 (2005).
218 Zustiak, S. P. & Leach, J. B. Hydrolytically degradable poly(ethylene glycol) hydrogel scaffolds with tunable degradation and mechanical properties. *Biomacromolecules* **11**, 1348-1357 (2010).
219 Kozlowski, M. T., Crook, C. J. & Ku, H. T. Towards organoid culture without Matrigel. *Communications biology* **4**, 1387 (2021).

Acknowledgements

Studies in the Fu research group are supported by the Michigan-Cambridge Collaboration Initiative, University of Michigan Mcubed Fund, University of Michigan Mid-career Biosciences Faculty Achievement Recognition Award, National Science Foundation (PFI-TT 2213845, I-Corps 2112458, CMMI 1917304, CBET 1901718, and CMMI 2325361), and National Institutes of Health (R21 NS113518, R21 HD100931, R21 HD105126, R21 NS127983, R21 HD109635, R21 HD105192, R33 CA261696, R01 GM134535, and R01 NS129850). The authors apologize to colleagues whose work they could not cite owing to space restrictions.

Author contributions

Y.L. and J.F. wrote the article text. Y.L. generated the figures. All authors contributed to the conceptualization of the article.

Competing interests

The authors declare no competing interests

Peer review information

Figures

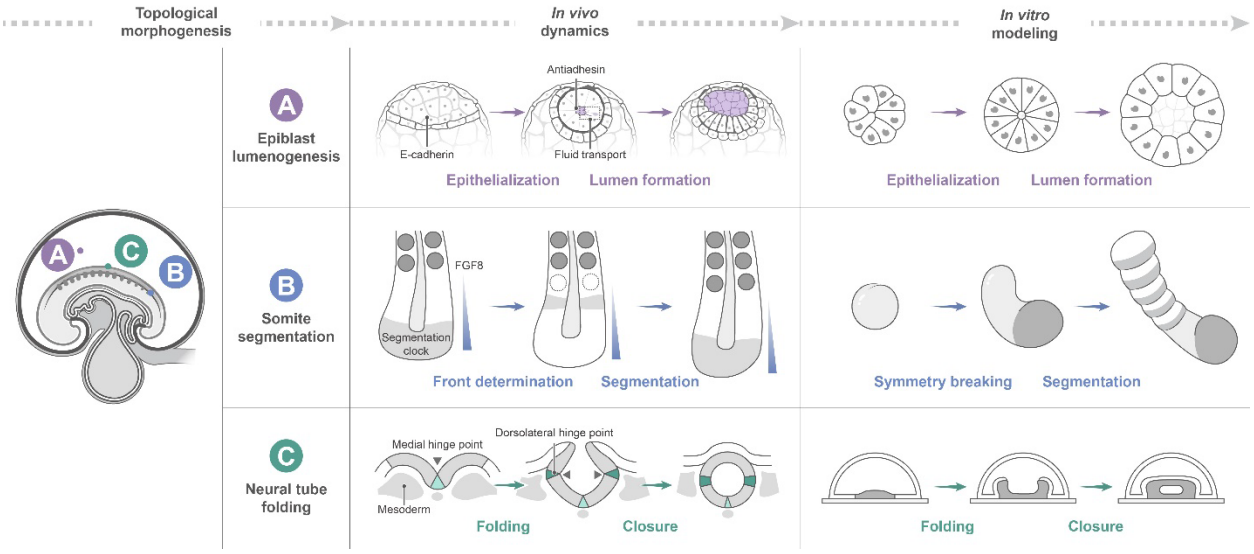

Fig. 1 | **In vivo knowledge and in vitro modeling of three topological morphogenetic events. a,** Epiblast lumenogenesis. **b,** Somite segmentation. **c,** Neural plate folding. Embryo schematics adapted with permission from Ref[2].

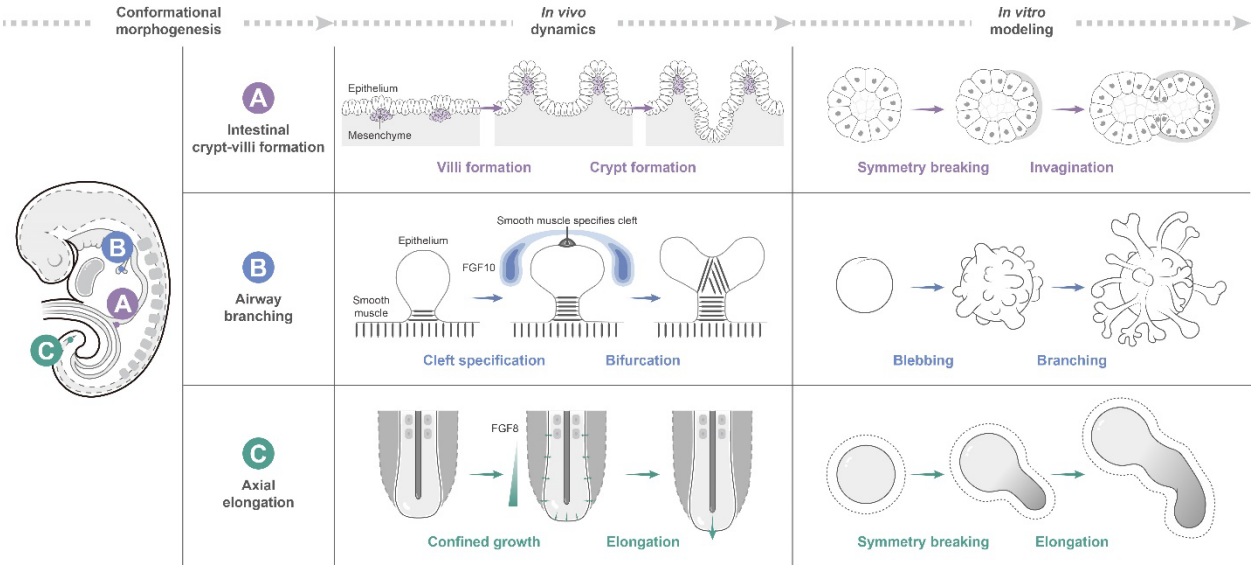

Fig. 2 | **In vivo knowledge and in vitro modeling of three conformational morphogenetic events. a,** Intestinal crypt-villi formation. **b,** Airway branching. **c,** Axial elongation. Embryo schematics adapted with permission from Ref[2]. Part **b** adapted with permission from Ref.[90]

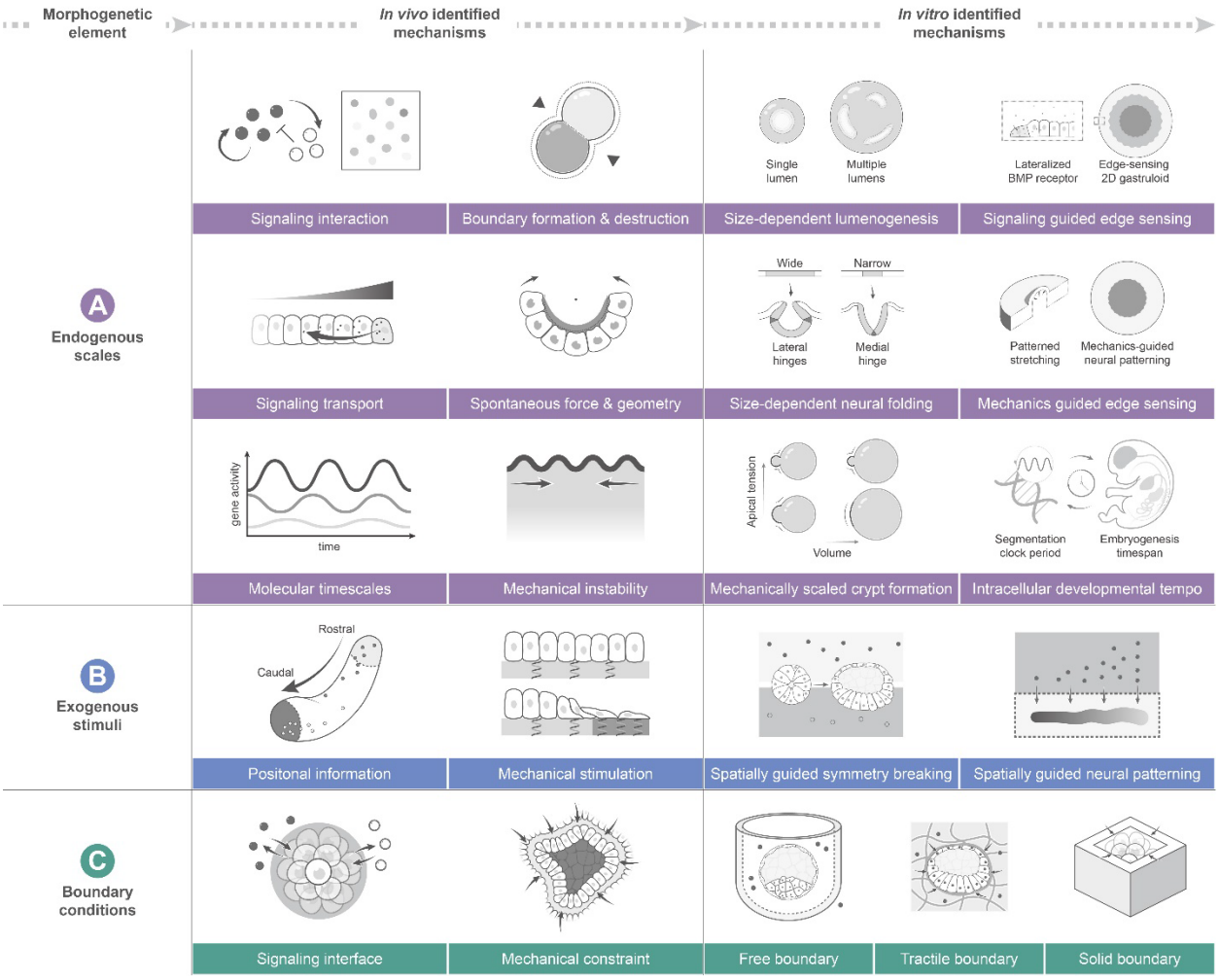

Fig. 3 | Essential aspects of morphogenetic dynamics with selected in vivo and in vitro examples. a, Endogenous morphogenetic scales. **b,** Exogenous stimuli. **c,** Boundary conditions. Part **a** adapted with permission from Ref.[2]

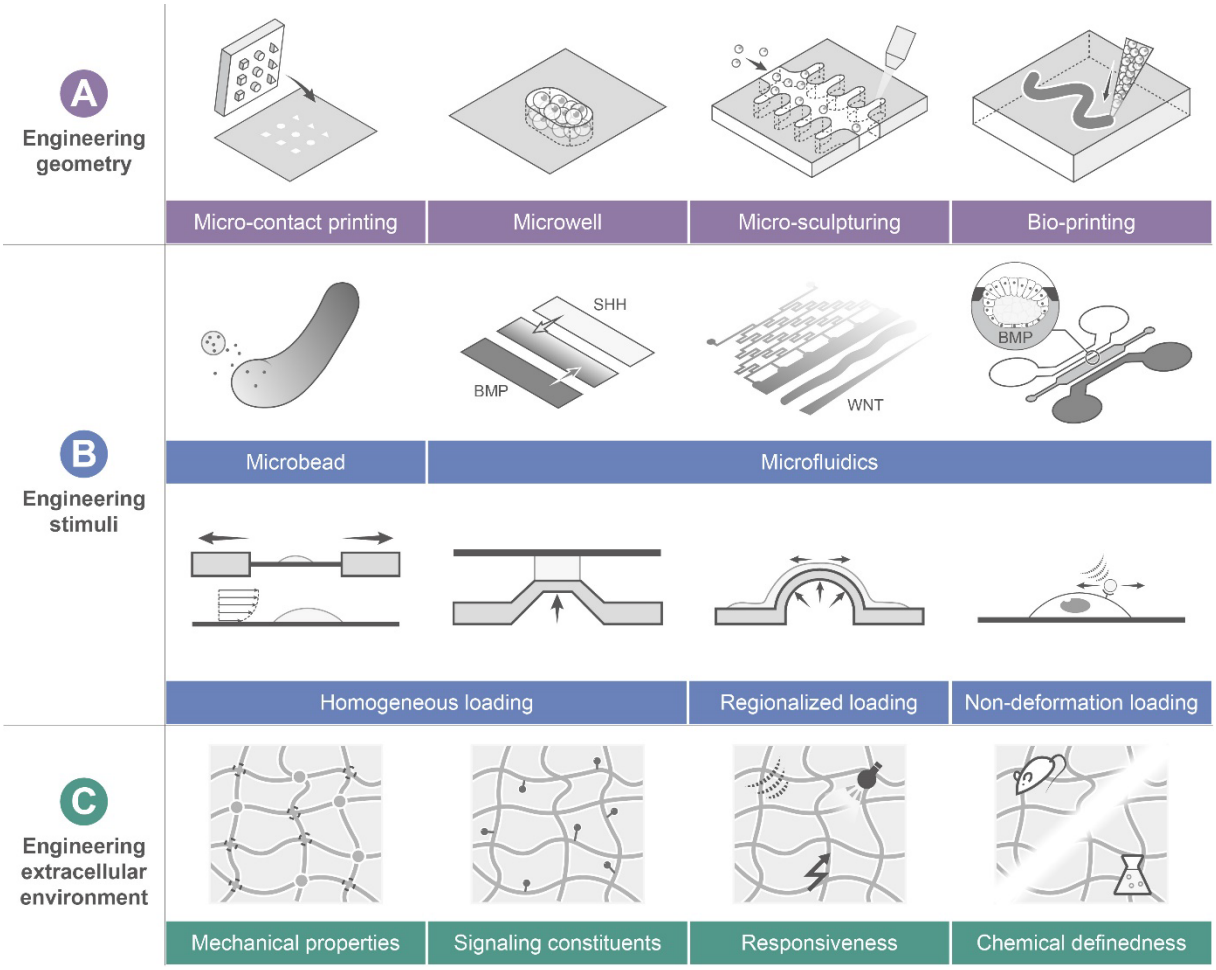

Fig. 4 | **Bioengineering tools and methods to model and study morphogenesis in vitro. a,** Modulation of tissue geometry. **b,** Application of exogenous stimuli. **c,** Modification of extracellular environment of embryoids and organoids.